STUDY OF ULTRAVIOLET ABSORPTION AND PHOTOCONDUCTION SPECTRA OF POLYIMIDE FILMS FABRICATED AT VARIOUS CURING TEMPERATURES

BY

LIN KAN

A Thesis

Submitted to the Faculty of Graduate Studies

in Partial Fulfillment of the Requirements

for the Degree of

MASTER OF SCIENCE

Department of Electrical and computer Engineering

University of Manitoba

Winnipeg, Manitoba

ISBN 0-315-85923-7

Canada

Name _____

Dissertation Abstracts International is arranged by broad, general subject categories. Please select the one subject which most nearly describes the content of your dissertation. Enter the corresponding four-digit code in the spaces provided.

Electronics and Electricity — SUBJECT TERM

0607 — SUBJECT CODE

U·M·I

Subject Categories

THE HUMANITIES AND SOCIAL SCIENCES

COMMUNICATIONS AND THE ARTS

Architecture 0729
Art History 0377
Cinema 0900
Dance 0378
Fine Arts 0357
Information Science 0723
Journalism 0391
Library Science 0399
Mass Communications 0708
Music 0413
Speech Communication 0459
Theater 0465

EDUCATION

General 0515
Administration 0514
Adult and Continuing 0516
Agricultural 0517
Art 0273
Bilingual and Multicultural 0282
Business 0688
Community College 0275
Curriculum and Instruction 0727
Early Childhood 0518
Elementary 0524
Finance 0277
Guidance and Counseling 0519
Health 0680
Higher 0745
History of 0520
Home Economics 0278
Industrial 0521
Language and Literature 0279
Mathematics 0280
Music 0522
Philosophy of 0998
Physical 0523
Psychology 0525
Reading 0535
Religious 0527
Sciences 0714
Secondary 0533
Social Sciences 0534
Sociology of 0340
Special 0529
Teacher Training 0530
Technology 0710
Tests and Measurements 0288
Vocational 0747

LANGUAGE, LITERATURE AND LINGUISTICS

Language
- General 0679
- Ancient 0289
- Linguistics 0290
- Modern 0291

Literature
- General 0401
- Classical 0294
- Comparative 0295
- Medieval 0297
- Modern 0298
- African 0316
- American 0591
- Asian 0305
- Canadian (English) 0352
- Canadian (French) 0355
- English 0593
- Germanic 0311
- Latin American 0312
- Middle Eastern 0315
- Romance 0313
- Slavic and East European 0314

PHILOSOPHY, RELIGION AND THEOLOGY

Philosophy 0422
Religion
- General 0318
- Biblical Studies 0321
- Clergy 0319
- History of 0320
- Philosophy of 0322

Theology 0469

SOCIAL SCIENCES

American Studies 0323
Anthropology
- Archaeology 0324
- Cultural 0326
- Physical 0327

Business Administration
- General 0310
- Accounting 0272
- Banking 0770
- Management 0454
- Marketing 0338

Canadian Studies 0385
Economics
- General 0501
- Agricultural 0503
- Commerce-Business 0505
- Finance 0508
- History 0509
- Labor 0510
- Theory 0511

Folklore 0358
Geography 0366
Gerontology 0351
History
- General 0578
- Ancient 0579
- Medieval 0581
- Modern 0582
- Black 0328
- African 0331
- Asia, Australia and Oceania 0332
- Canadian 0334
- European 0335
- Latin American 0336
- Middle Eastern 0333
- United States 0337

History of Science 0585
Law 0398
Political Science
- General 0615
- International Law and Relations 0616
- Public Administration 0617

Recreation 0814
Social Work 0452
Sociology
- General 0626
- Criminology and Penology ... 0627
- Demography 0938
- Ethnic and Racial Studies 0631
- Individual and Family Studies 0628
- Industrial and Labor Relations 0629
- Public and Social Welfare 0630
- Social Structure and Development 0700
- Theory and Methods 0344

Transportation 0709
Urban and Regional Planning 0999
Women's Studies 0453

THE SCIENCES AND ENGINEERING

BIOLOGICAL SCIENCES

Agriculture
- General 0473
- Agronomy 0285
- Animal Culture and Nutrition 0475
- Animal Pathology 0476
- Food Science and Technology 0359
- Forestry and Wildlife 0478
- Plant Culture 0479
- Plant Pathology 0480
- Plant Physiology 0817
- Range Management 0777
- Wood Technology 0746

Biology
- General 0306
- Anatomy 0287
- Biostatistics 0308
- Botany 0309
- Cell 0379
- Ecology 0329
- Entomology 0353
- Genetics 0369
- Limnology 0793
- Microbiology 0410
- Molecular 0307
- Neuroscience 0317
- Oceanography 0416
- Physiology 0433
- Radiation 0821
- Veterinary Science 0778
- Zoology 0472

Biophysics
- General 0786
- Medical 0760

EARTH SCIENCES

Biogeochemistry 0425
Geochemistry 0996
Geodesy 0370
Geology 0372
Geophysics 0373
Hydrology 0388
Mineralogy 0411
Paleobotany 0345
Paleoecology 0426
Paleontology 0418
Paleozoology 0985
Palynology 0427
Physical Geography 0368
Physical Oceanography 0415

HEALTH AND ENVIRONMENTAL SCIENCES

Environmental Sciences 0768
Health Sciences
- General 0566
- Audiology 0300
- Chemotherapy 0992
- Dentistry 0567
- Education 0350
- Hospital Management 0769
- Human Development 0758
- Immunology 0982
- Medicine and Surgery 0564
- Mental Health 0347
- Nursing 0569
- Nutrition 0570
- Obstetrics and Gynecology .. 0380
- Occupational Health and Therapy 0354
- Ophthalmology 0381
- Pathology 0571
- Pharmacology 0419
- Pharmacy 0572
- Physical Therapy 0382
- Public Health 0573
- Radiology 0574
- Recreation 0575
- Speech Pathology 0460
- Toxicology 0383

Home Economics 0386

PHYSICAL SCIENCES

Pure Sciences

Chemistry
- General 0485
- Agricultural 0749
- Analytical 0486
- Biochemistry 0487
- Inorganic 0488
- Nuclear 0738
- Organic 0490
- Pharmaceutical 0491
- Physical 0494
- Polymer 0495
- Radiation 0754

Mathematics 0405
Physics
- General 0605
- Acoustics 0986
- Astronomy and Astrophysics 0606
- Atmospheric Science 0608
- Atomic 0748
- Electronics and Electricity 0607
- Elementary Particles and High Energy 0798
- Fluid and Plasma 0759
- Molecular 0609
- Nuclear 0610
- Optics 0752
- Radiation 0756
- Solid State 0611

Statistics 0463

Applied Sciences

Applied Mechanics 0346
Computer Science 0984
Engineering
- General 0537
- Aerospace 0538
- Agricultural 0539
- Automotive 0540
- Biomedical 0541
- Chemical 0542
- Civil 0543
- Electronics and Electrical 0544
- Heat and Thermodynamics ... 0348
- Hydraulic 0545
- Industrial 0546
- Marine 0547
- Materials Science 0794
- Mechanical 0548
- Metallurgy 0743
- Mining 0551
- Nuclear 0552
- Packaging 0549
- Petroleum 0765
- Sanitary and Municipal 0554
- System Science 0790

Geotechnology 0428
Operations Research 0796
Plastics Technology 0795
Textile Technology 0994

PSYCHOLOGY

General 0621
Behavioral 0384
Clinical 0622
Developmental 0620
Experimental 0623
Industrial 0624
Personality 0625
Physiological 0989
Psychobiology 0349
Psychometrics 0632
Social 0451

STUDY OF ULTRAVIOLET ABSORPTION AND PHOTOCONDUCTION SPECTRA OF POLYIMIDE FILMS FABRICATED AT VARIOUS CURING TEMPERATURES

BY

LIN KAN

A Thesis submitted to the Faculty of Graduate Studies of the University of Manitoba in partial fulfillment of the requirements for the degree of

MASTER OF SCIENCE

ABSTRACT

The absorption and photoconduction spectra in the ultraviolet region for PMDA-ODA polyimide films fabricated under various curing temperatures have been measured. There are four absorption peaks located at 3.65 eV, 4.35 eV, 5.65 eV and 6.40 eV in the fully cured polyimide films. The peak at 6.40 eV is practically independent of the curing temperature, but the other three peaks increase with increasing curing temperature.These four peaks are due to intra- and intermolecular optical transitions. In the photoconduction quantum efficiency spectra, there are also four peaks in the fully cured polyimide films but they are located at 3.55 eV, 4.05 eV, 4.90 eV and 5.80 eV. Analysis of the photoconduction quantum efficiency spectra yields values of 4.17 eV and 4.37 eV as the potential barrier heights for photoemission from Au and Ag electrodes to polyimide, respectively. The quantum efficiency increases with increasing applied electric field, following closely the Onsager theory with a thermalization separation 30 $\AA$ in the UV region. The primary yield increases with increasing curing temperature.

ACKNOWLEDGMENTS

The author would like to extend his sincerest thanks to his advisor Prof. K. C. Kao for his constant support and guidance throughout the course of this study. The author is also indebted to his colleagues and fellow students at the Materials and Devices Research Lab for their stimulating discussions and technical assistance, particularly D. Liu, T.T. Chau, S. R. Mejia, and M. Jing.

More personally, the author wishes to thank G. Rosendahl for his friendship, encouragement, and help during this study.

Contents

Chapter 1

Introduction

Polymers are increasingly being used in a wide variety of applications in electronics and photonics. The traditional applications of polymers may be considered "passive" in the sense that they do not play an important role in active devices or circuits, such as circuit boards, wire and cable insulation and adhesives. However, technology now has reached a point that the unique properties of polymers can be made suitable not only for the "passive" applications, but also for the "active" applications. Examples of such applications include conducting polymers, nonlinear optic devices, sensors and molecular electronic devices.

Polyimide is one of such polymers which can be used as a passive or an active element. This polymer is formed by imidization of its polyamic acid precursor. The molecular structures of polyimide therefore change with the curing temperatures, which provides a way to study the relations of electrical and optical properties of the

polyimide with its molecular structures. Previous studies focus on the effects of curing temperature on the physical properties, such as dielectric constant, adhesion, crystallinity and etch rate. Since the applications of polyimide continue expanding into new areas, an understanding of the relation between the electrical and optical properties of polyimide and its molecular structures becomes very important, especially for "active" applications. One of the objectives of the present study is to study the relation between the optical absorption spectra and the molecular structures of polyimide. The details of this part of studies are given in chapter 3.

Polyimide falls into the class of electron donor-acceptor polymers. It has been reported[1] that addition of electron donors to PMDA-ODA polyimide films results in an enhancement of the photocurrent due to the formation of the charge-transfer complexes between the added electron donors and the polyimide. However, little has been reported concerning the formation of charge-transfer complexes by polyimide itself. Thus the investigation of the role of charge transfer complexes in photoconduction in UV region forms another objective of this study. This is given in chapter 4.

Much of the driving force behind the research and development of polyimide materials comes from their elctronic and photonic applications. A great deal of work now is available in the literature

and many new promising applications have been continuously put forward. Hence a review of the properties and applications of polyimide is given in chapter 2. Final conclusions resulting from this study are given in chapter 5.

Chapter 2

Review of the Properties and the Applications of Polyimides

Polyimides have become one of the most important polymers for electronic and photonic applications due to their high purity, high heat resistance, excellent dielectric properties and easy to process.[2–4] In this chapter, the properties and the applications of polyimides will be briefly reviewed.

2.1 Physical and Electrical Properties of Polyimides

Polyimide films have already been used as dielectric layers for integrated circuits, α-ray shieldings, buffer coatings and photoresists.[5,6] The physical properties of polyimide have been extensively investigated during the past decade.[7,8] Polyimides are formed by imidization of their precursors. The degree of imidization is dependent on the curing temperature. The physical properties such as etch rate

and pattern profile are therefore dependent on the heat-treatment. The crystallinity increases and the etch rate decreases with the increase of the curing temperature. The dissipation factor D is a sensitive indicator of the cure conditions, and its value is dependent on the curing temperature. D decreases with the increase of curing temperature and curing time at temperatures lower than 300 ^oC due to solvent (H_2O) release and imidization. To achieve the absolute minimum value of D, it is necessary to bake the polyimide film between 350^oC and 450^oC in nitrogen gas. This high baking temperature drives out H-bonded water. The minimum D at 1 MHz achierable under these conditions is about 0.003 for DuPont PI2545 polyimide. D will increase if temperature is futher increased as decomposition starts to occur. The dielectric constant is 3.2 at 1 MHz for fully cured polyimide as compared to 3.8 for sputtered SiO_2. This lower dielectric constant of polyimide is an advantage over SiO_2.

Polyimides can be used under temperatures up to 300^oC. It is known that the viscosity of polyimide precursor (polyamic acid) is reduced by the absorption of a small amount of water. This is because the absorbed water reduces the molecular weight by hydrolysis. It has been found that even a small amount of water in polyamic acid solution would greatly reduce the heat resistance of

polyimides. The influence of water on heat resistence is considered to be as follows: Moist acid dianhydrides contain free acids. When polyimides are thermally cured, free acids are converted into corresponding dianhydride monomers and then evaporate. Since the free acids do not take part in polymerization, they prevent high polymer formation and reduce the heat resistance. Therefore, it is very important to keep the polyimide precursor materials dry.

One of the most important properties of the thin polyimide films for applications is their high adhesion to the semiconductor materials and metals. The adhesion of polyimide to Si and SiO_2 surfaces is good, But after prolonged exposure to electrical stressing, it tends to degrade. The Du Pont VM651 promoter can improve the long-term stability of polyimide-SiO_2 and polyimide-Si interfaces. Polyimide has a good adhesion to aluminum surface, but a relatively poor adhesion to copper. However, if a thin film of chromium is deposited first, adhesion to copper can be dramatically improved.[9] The interaction between the PMDA-ODA polyimide surface and chromium atoms has been investigated extensively.[10–12] The reaction takes place in several stages and is chromium-coverage-dependent. In the first stage, initial electron transfer from the chromium to the polyimide occurs with a very small amount of chromium atoms. This transfer results in the formatiom of polyimide radical anion

species. In these species the unpaired electrons are delocalized over the dianhydride portion of the polyimide, but are not appericiably delocalized over the diamine portion. Following polyimide reduction by the chromium, a second stage of the reaction occurs with continued depositon of chromium. This phase of reaction results in the formation of chromium nitride, oxide, and carbide species. Initial reduction of polyimide may activate the polymer toward the formation of these species. Either the formation of the chemical bonds between the metal and the polyimide or the alteration of the polyimide surface to improve mechanical interactions may give rise to the observed improved adhesion.

The primary function of polyimides is used as insulating layers between conducting parts. The electrcal properties of polyimides are obviously of great importance in their applications to integrated circuit fabrication. Even very small amount of charge transport or storage in multilevel insulating structures may cause a great change in the electrical characterstics of underlying devices, which could result in poor circuit performance or failure. At a typical electrical field of 5×10^5 v/cm, the conductivity of polyimide is about $10^{-16}\Omega^{-1}cm^{-1}$ which is close to that of thermal SiO_2. But at higher fields such as 2×10^6 v/cm, the conductivity of polyimide is increased to about $3 \times 10^{-13}\Omega^{-1}cm^{-1}$ which is several orders larger

than that of thermal SiO_2. The electrical breakdown strength is thickness dependent. For a typical value of 1-2 μm for interlevel insulating layers, the breakdown strength is about 6×10^6 v/cm which is adequate for most applications. Sodium contamination has long been a major reliability concern in silicon device processing. The sodium barrier properties of insulating films for device fabrication are of great importance in shielding the underlying oxides and pn junctions from sodium contamination. Polyimide, once cured, provides an effective sodium ion barrier for underlying oxide. But special attention should be paid to avoid ion contamination during polyimide film deposition and curing.

2.2 The Electronic Structure of PMDA-ODA Polyimide

In order to understand the electron and energy transfer mechanisms in polyimide, an understanding of the electronic structure is important. The entire valance-band density of states(VBDOS) has been measured using high-resolution photoelectron spectroscopies including x-ray photoelectron spectroscopy, soft-x-ray photoelectron spectroscopy and ultraviolet-photoelectron-spectroscopy.[13,14] The theoretical VBDOS has also been calculated on the basis of the Nicolas-Durand valence-effective-hamiltonian(VEH) model.[15] The calculated

values are in good agreement with the experimental results. Figure 2.1 shows the VEH calculation of the VBDOS for polyimide. The entire spectrum is divided into six different energy regions so that the states in the respective regions are of similar origin. The origins of VBDOS are listed in table 2.1 for polyimide. The states at the high-binding-energy side of the valence-band spectra of polyimide are typically monatomic and localized on particular subunits of the whole system. For example, the C 2s orbitals of the benzene rings do not mix substantially with the C 2s orbitals of the carbonyl groups. This property is essential, since, by studying the changes in the VB-DOS due to interactions of the polyimide with, e.g., metals, useful information concerning the particular sites involved in interfacial interactions can be obtained from the photoelectron spectroscopy. The regions D and E of intermediate binding energies have high densities of states originating from σ states, including mixtures of 2s-2p, 2p-2p, and 2p-1s atomic orbitals. Therefore, individual states become less well resolved. The low-binding-energy region of the valence-band spectra contain σ and π states as well as oxygen and nitrogen lone-pair states. The one at the low-binding-energy side is dominated by the π states and that at the high-binding-energy side contains the lone-pair states. The electron and energy transfers in the UV region are believed to involve the π states.

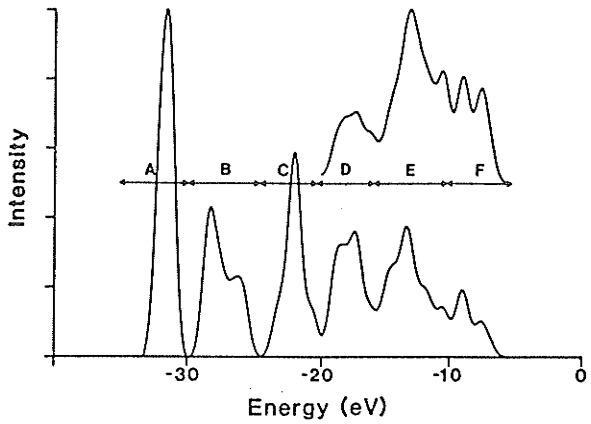

Figure 2.1: The VEH calculation of the VBDOS for polyimide.

Table 2.1 The Origins of VBDOS of Polyimide

Energy Region	**Origins of VBDOS**
A (-35 to -30 eV)	O 2s atomic orbitals
B (-30 to -24 eV)	mainly N 2s, with some 2s from C-O and C-N
C (-24 to -20 eV)	C 2s from the phenyl ring and 2pσ from C-O, C-N
D (-20 to -16 eV)	mainly 2pσ states with some σ states from C-H
E (-16 to -10 eV)	extended σ states, oxygen lone-pair states
F (above -10 eV)	extended π states and N,O lone-pair states

The energy gap(E_g), ionization potential(IP) and electron affinity(EA) are crucial for the understanding of the electron-transfer capabilities in the polyimide. The IP indicates whether a given acceptor is capable of ionizing the polymer chains. The E_g determines the probability of electrons transfer from the velence band directly to the conduction band. The EA substracted from the IP, determine what impurities can be used as dopants to make n-type polyimide.

The calculated IP of PMDA-ODA polyimide ranges from 8.0eV[16] to 8.97eV[17], and the experimental value is 9.1eV.[18] The electron affinity(EA) and energy gap(E_g) are estimated to be -2 eV and 7 eV, respectively.

2.3 Photoconduction in Polyimides

Photoconduction in polyimide was first reported by M. Ieda et. al.[19] They have reported that two photocurrent peaks at 2.70 eV and 3.65 eV are independent of electrode materials and applied voltage polarities. The photocurrent increases with the reduction in molecular ordering observed by X-ray diffraction, which indicates that the magnitude of the photocurrent in polyimide is closely related to its molecular structure. Although the photoconductivity in polyimide has been investigated, its use as a photoconductive material is limited by its low quantum yield of photogenerated charge carriers. Sensitization of photoconductivity in electron-donating polymers by the addition of electron acceptors has been reported,[20] with most of the focus on poly(N-vinyl-carbazole)(PVK). Resently, Freilich[1] has reported photoconductivity in electron-donor-loaded polyimide films. These films are characterized by their high photocurrent gains achieved without significantly sacrificing other positive features of polyimide. For example, the addition of N,N-

dimethylaniline(DMA) electron donors to polyimide films results in an increase in photocurrent by four orders of magnitude as compared to the pure polyimide. This increase in photocurrent is due to the absorption of the light energy by the charge-transfer complexes formed between the added electron donors and the imide portions of the polyimide backbone. Ultraviolet absorption spectra of fully cured PMDA-ODA polyimide and a series of polyimide model compounds have also been studied. Those compounds are meant to model the chemical fragments of the polyimide system in an effort to understand the contributions made by each fragment. The CNDO/S3 computational model has been used to provide a quantitative description of the spectra. The absorption bands in PMDA-ODA polyimide are associated with intramolecular charge transfer π-π^* transitions. The measured PMDA-ODA polyimide absorption spectrum is in good agreement with the computed spectrum excepting that the measured absorption peak at 5.9eV is missing in the computed spectrum. This deviation is attributed to a possible artifact of the computation resulting from the empirical nature of the chosing parameters used in the CNDO/S3 model for polyimide.[21]

2.4 Polyimides for Microelectronic Applications

2.4.1 The Use of Polyimide as the Interlevel Dielectric layers of the Multilevel Structure

A multilevel structure consisting of alternating metal and dielectric layers is necessary for the interconnection in high density or VLSI circuits. The interlevel dielectric layers of the multilevel structure must have the following functions: (1) They must provide planarization of the underlying topography while allowing high resolution patterning of via holes necessary for the contact between metal layers. (2) They must provide insulation integrity. (3) They must contribute minimally to device capacitance. A number of materials can be used for such dielectric layers. The principle reasons using polyimide are: (1) Polyamic acids, the precursors of polyimide, are solvent-soluble to form a viscous liquid that can be spun onto a wafer to create a relatively planar surface that is suitable for the next level metallization. (2) The cured polyimide coating has excellent electronic properties and heat resistance. It also provides excellent mechanical protection. (3) Polyamic acid coating solution can be spun, exposed, and etched with conventional experimental equipment.

Deposited SiO_2 films have been used as interlevel dielectric layers in the multilevel structure for quite some time. However, with

this construction, reliability and yield become problems due to the topography of metal edges and via holes or oxide windows for interlayer connections. Polyamic acid can be made a viscous liquid which can flow into the cavities and produce a relativity flat surface for the next level metallization. The comparison for a two-level metallization structure of the conventional SiO_2 method and the planar metallization with polyimide technology is shown in Fig.2.2. Since multilevel metallization is the key to the fabrication of VLSI circuits, this application can be considered as the greatest value-in-use among polyimide applications in microelectronics.

The high-quality ultrathin polyimide films have been prepared by using Langmuir-Blodgett(LB) thchnique. The reported possible applications of Polyimide LB films include metal/PILB/metal tunnel junctions, Nb-Au/PILB/Pb-Bi superconductor Josephson junctions,[22] and surface-stablized ferroelectrc liquid crystal.[23] Polyimides have also been used as the buffer coating to protect semiconductor devices against external stresses acting upon their surfaces, the alpha ray shielding for DRAM, high-speed bipolar devices, and the high desity package materials,[24] etc.

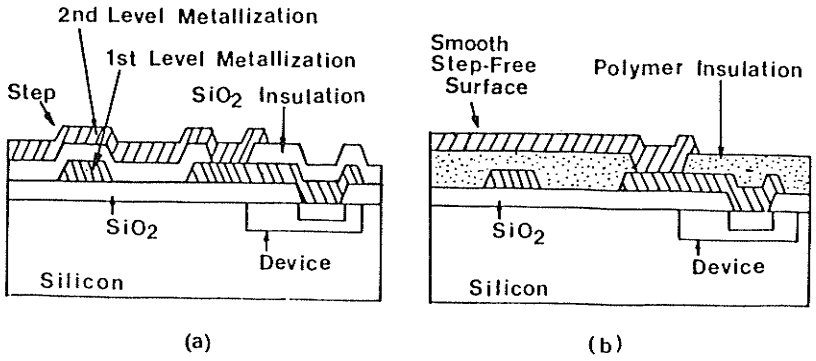

Figure 2.2: Comparison of two-level metallization structure by

(a) conventional method and (b) polyimide technology.

2.4.2 The Use of the Photosensitive Polyimide as the Photoresist and Dielectric Material

Integrated circuit(IC) fabrication requires the selective diffusion of tiny amounts of impurities into specific regions of the silicon substrate to produce the desired electrical characteristics of the circuit. These regions are defined by lithographic processes that consist of two steps: (1) Delineation of the desired circuit pattern in a photoresist layer. (2) Transfer of that pattern via processes such as etching into the underlaying substrate. In the conventional lithographic processes, the photoresist is removed after etching, baring the patterned oxide that serves as a mask during subsequent high

temperature diffusion of dopants into the exposed silicon substrate. By the introduction of photosensitive polyimide, however, the photoresist is left behind to become an insulating layer in multilayered ICs thus reducing the process steps and increasing the reliability. The exposure and cure process of photosensitive polyimide is shown in Fig.2.3 and the processes used in manufacturing two-level metallization devices by using polyimide and photosensitive polyimide are shown in Fig.2.4.[25]

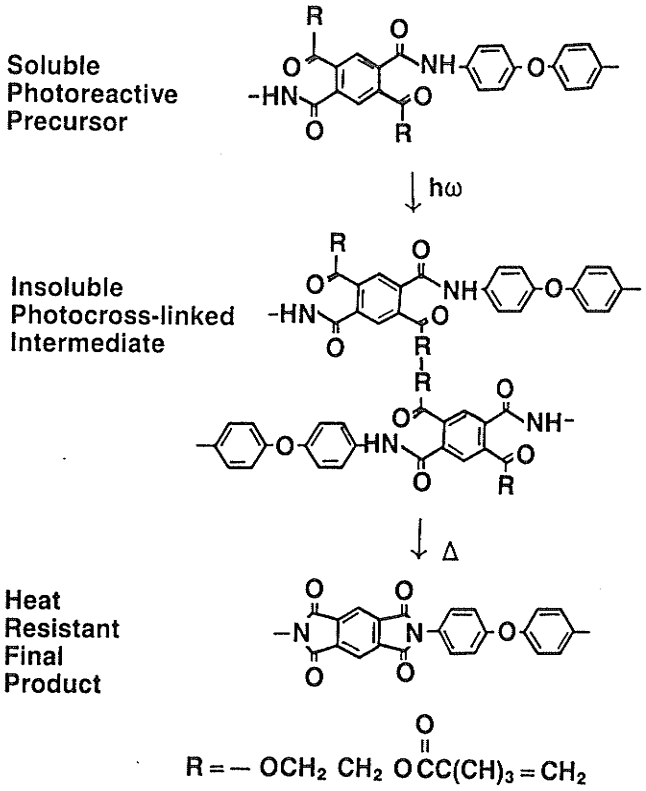

Figure 2.3: The exposure and cure process of photosensitive polyimide.

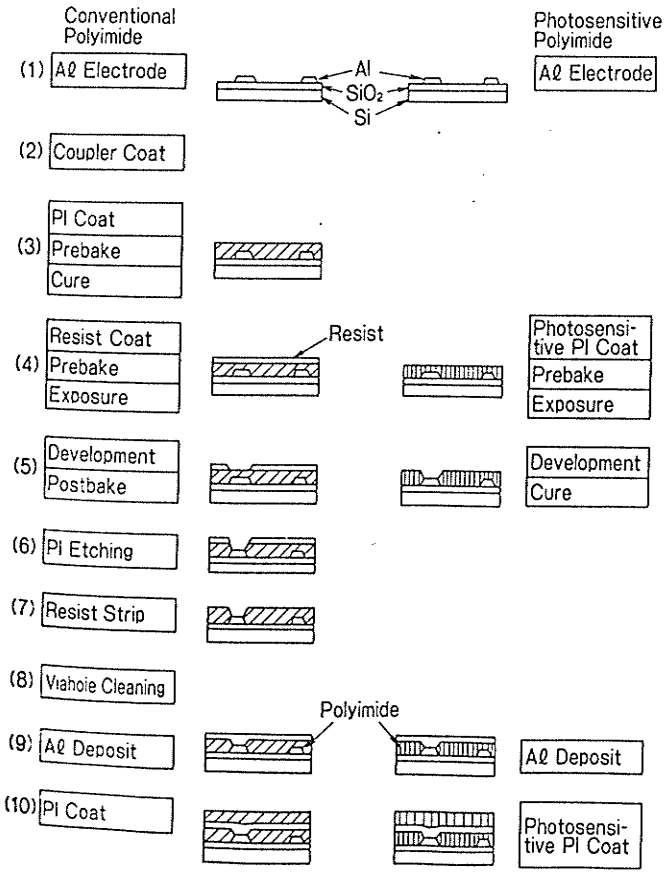

Figure 2.4: Flow chart of the fabrication process for polyimide interconnection of two-level metallization devices using polyimide and photosensitive polyimide.

2.5 Polyimides for Photonic Applications

The inventions of lasers and optical fibers have had a profund influence on modern society, particularly in the processing and transport information. The driving forces behind photonic applications are the enormous capacity and high speed. The all optical switches for telecommunication and the optical waveguides for higher-speed interchip communication are two such good examples. As will be shown in the following brief discussion, polyimide plays an important role in this rapidly expanding area.

2.5.1 The use of polyimide as the Waveguide Material in Integrated Optics

The concept of integrated optics is that in all of the elements and interconnections, the optical signals are confined in compact optical waveguides. The construction of an optical waveguide in the surface of a substrate requires alteration of the refractive index of the region, so light can be guided or channeled. These guides are then used both to form the various circuit elements and to make interconnections between elements. In the case of three-dimensional waveguides, the refractive index differential required between the guide and its surroudings depends on the sharpest bend through which light must be traveled by the guide. A 1% increment gen-

erally is sufficient for most purposes. Polyimide is well suited for waveguide fabrication because its final structure depends on curing processes. Therefore its refractive index will be different at each thermal or optical curing stage.[26] The polyimide waveguide fabrication methods include laser writing by thermal curing, laser writing with visible radiation in photosensitive polyimide, photolithography by contact printing and electron beam lithography.[27] The attenuation loss values below 0.5 db/cm for polyimide have been obtained using optimized curing conditions. Polyimide waveguides integrated with silicon-based devices have been recently reported.[28]

2.5.2 The Use of Polyimide as an Electrooptic(EO) Material

In the field of photonics, the applications of polyimide as "passive" optical waveguide is already being heavily pursued. Polyimide serves some structural, protective, or guiding function but is not integral to the functioning of a device. For active applications, however, some types of nonlinear optical response are required when the material is irradiated with light of very high intensity, usually from a laser. Nonlinear optics is concerned with the interactions of electromagnetic fields with materials to produce new fields which can be altered in phase, frequency, amplitude, or other propagation characteristics from the incident fields. The polarization(P) induced

in a medium by an external electric field(E) can be expressed as:

$$P = a_1 E + a_2 E^2 + a_3 E^3 + ... \tag{2.1}$$

where a_2, a_3 are hyperpolarizabilities which are responsible for the nonlinear response of the materal to the impinging radiation.

The electrooptic(EO) or Pockles effect occurs due to the interaction between an optical field and a direct current field in the nonlinear medium, altering the propagation characteristics of the light. Poled EO polymer thin films have been emerged in the photonics as a new class of EO materials. The processes used to form thin films from polymer EO materials, such as spin or dip coating techniques, do not usually produce EO films since the bulk structure is still centrosymmetric. A molecular alignment process, such as electrically induced poling, is needed to establish a noncentrosymmetric structure. Figure 2.5 shows the poling process with two different electrode geometries.[29] Before the poling step, the active molecules in the EO layer are randomly oriented. After poling, the active molecules are partially ordered in areas defined by the electrodes. The net alignment of molecular dipoles induced by the electric field poling of a polymer system doped with nonlinear optical(NLO) guest molecules gives rise to a linear EO effect. In this way, it is possible to make high-speed active EO polymer waveguide devices including, for example, phase modulators, directional cou-

plers, and Mach-Zehnder interferometers.[30]

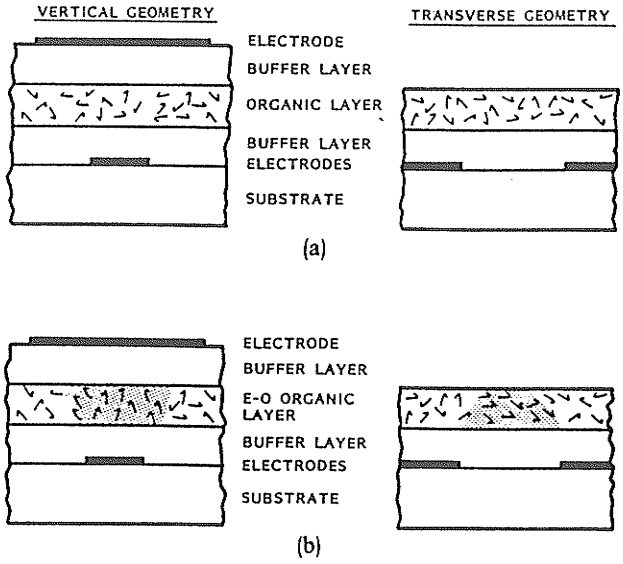

Figure 2.5: Waveguide device structures (a) before and (b) after the poling.

In device applications, most of the organic EO systems which have been known[31] not suitable for real device fabrication due mainly to the failure to meet the thermal stability requirement dictated by the temperature cycles during the standard semiconductor process. However, this kind of thermal requirement can be met by polyimide which already receives wide use in the microelectronic industry. It is found that the thermal stability of the EO polyimide system is largely dependent on the curing process.[32] High-temperature densification curing at 360°C is essential in realizing a thermally stable EO response at high temperatures. A thermally stable EO response at 200° for 80 hours and at 300° for 2 hours has been obtained in a

Erythrosin/Polyimide guest-host system.[33]

2.6 A Polyimide-Based Humidity Sensor

Most of the humidity sensors can be classified as follows based on their operating mechanisms: those which respond to electrical change such as resistance or capacitance; thoses which measure mechanical property changes of a film or a filament; and those which are based on psychrometic measurements by comparing the latent heat of evaporation of a saturated enviroment to the enviroment in question. Polyimide is moisture-sensitive which in fact is regarded as one of its major disadvantages when it is used as an interlevel insulating material for microelectronic applications. The sensing mechanism of polyimide is based on the fact that the dielectric constant of polyimide is linearly related to the ambinent relative humidity. Therefore, the capacitance of a paralled plate device using polyimide as the dielectric material is a linear function of the ambinent relative humidity because polyimide does not swell during moisture absorption. Polyimide has been widely used in integrated circuit fabrication as an interlevel dielectric layer, passivation layer, α-ray shielding and planarizer. Standard integrated circuit processing techniques can easily be adopted to fabricate such PI based miniaturized sensors. The dielectric constant of a mixture is given

by

$$\epsilon = [V_2(\epsilon_2^{1/3} - \epsilon_1^{1/3}) + \epsilon_1^{1/3}]^3 \tag{2.2}$$

where ϵ_1 and ϵ_2 are the dielectric constants of polyimide and water, which are about 3.5 and 80, respectively. V_2 is the fractional volume of the water absorbed. The more the water is absorbed, the larger is the dielectric constant of the mixture. Figure 2.6 shows the top view and the cross section of a polyimide humidity sensor device.[34] The capacitance measured at 1 kHz as a function of ambient RH is shown in Fig.2.7. The sensitivity of the sensor to moisture is quite high. The capacitance is increased by 35% from 0 to 100%RH. The response time of the sensor consists of absorption and desorption time, which is controlled by the moisture diffusion process. The desorption time is usually much larger than the absorption time and depends mainly on the upper finger electrode width because it takes longer time to remove the residual water trapped in the metal-polyimide interface. If a more rapid response is desired, the upper electrode should be patterned with a smaller finger width. A simple one-dimensional diffusion model predicts that the equilibrium time is proportional to the square of the finger width. In order to achieve a higher sensitivity, a thinner polyimide film should be used so that a larger change in capacitance with relative humidity can be obtained.

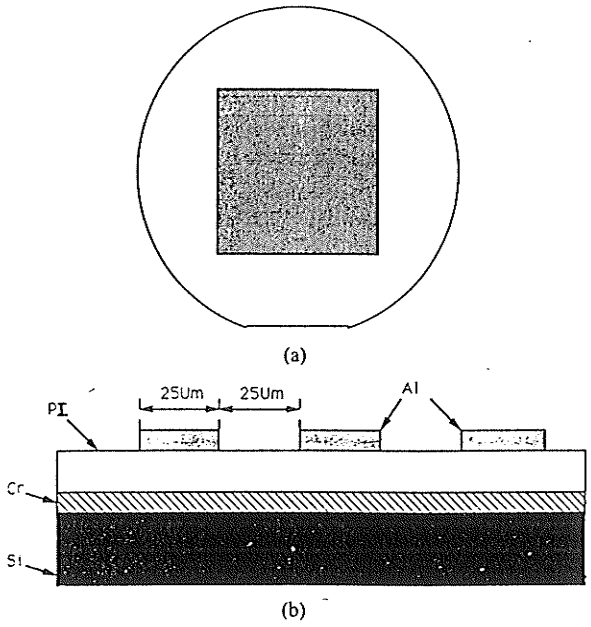

Figure 2.6: (a) Top view of polyimide sensor device.

(b) Cross section of polyimide sensor device.

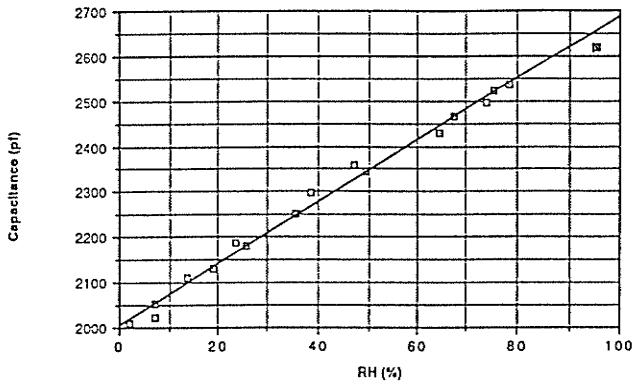

Figure 2.7: Capacitance versus ambient RH for the parallel plate polyimide sensor.

Chapter 3

Infrared and Ultraviolet Absorption Spectra of PMDA-ODA Polyimide Films at Various Curing Temperatures

The recent discoveries of the laser ablation process[35,36] and the ability to form electron donor-acceptor charge complexes make polyimide very attractive in microelectronic and photonic applications. A great deal of work, both experimental and theoretical, has been reported in the past decade about this material.[37–42] Analysis based on X-ray photoelectron spectroscopy (XPS), soft-X-ray photoelectron spectroscopy(SXPS),and ultrovolet photoelectron spectroscopy (UPS) has provided detailed information about the electronic states of polyimide in a wide energy range from the ground state up to the excited states in the ultraviolet(UV) region, as well as its electronic structure.[17,18] But little information has been reported about the charge and energy transfer processes above the valence band,

especially their relations with the curing temperatures.

The polyimide materials are usually formed by imidization of their polyamic acid precursors. It is well known that the molecular structures of polyimides are sensitive to the curing temperatures. In this chapter, we shall describe the PMDA-ODA polyimide sample preparing processes and the use of infrared(IR) spectra for characterizing polyimide samples at various curing temperatures used for our experiments. We shall present the measured ultraviolet(UV) absorption spectra of PMDA-ODA samples fabricated at various curing tempratures. On the basis of the relations between changes of the absorption spectra and changes of the chemical and physical structures during the cure, the energy transfer and optical absorption processes in the UV region will be discussed.

3.1 Experimental Techniques

3.1.1 For Infrared Measurement

The polyimide films used for this investigation were fabricated using Du Pont PI2545 pyromellitamic dianhydride-oxydianiline(PMDA-ODA) and Du Pont T-9039 thinner. The PMDA-ODA was diluted with the thinner to form a solution with a suitable viscosity. This solution was then spin-coated onto the substrates. By controlling the spin speed or the dilution of the PMDA-ODA with thinner, a

range from 500 $\AA$ to 5 μm in sample thickness could be obtained. The mixed polyimide solutions were stored at temperatures below 4 ^oC. In order to avoid the moisture condensation, the mixed solution should be brought to room temperature before opening the container. Otherwise, moisture would attack and degrade the polyamic acid polymer. The polyimide samples were thermally cured for 30 min in air at each of the following curing temperatures, 100 ^{o}C, 135 ^{o}C, 150 ^{o}C and 200 ^{o}C. For curing temperatures above 200 ^{o}C, polyimide samples were cured in nitrogen for 60 min at each curing stage. The degree of imidization was determined by the comparison of the IR absorption peak of the polyimide with that having a 100% imidization, which will be described in section 3.2. For IR absorption measurements the substrates used were $< 100 >$ oriented, p-type, 60 Ω-cm silicon wafers and the Bomen Michelson-100 infrared spectrometer was used for the measurements.

3.1.2 For Ultraviolet Measurement

The PMDA-ODA polyimide thin films were prepared by spinning Du Pont PI2545 onto optical quartz substrates. The PI film thickness was measured using the Dektak surface profile unit and the measured values were consistent with those obtained from ellipsometric measurements. Table 3.1 summarizes the parameters of the

typical polyimide samples used for experiments being reported.

Table 3.1 The typical PI samples used for absorption measurement

Sample	Thickness(μm)	Curing Temperature(^{o}C)	Imidization(%)
a	0.078	135	10
b	0.071	150	67
c	0.064	200	96
d	0.060	350	100

The ultraviolet absorption spectra were measured using a Cary 14 spectrophotometer. A simplified diagram of the optical and photometric system is shown in Fig.3.1. The polyimide sample was put in the sample cell and a blank quartz substrate was put in the reference cell. Energy from a suitable source enters the monochromator through an entrance slit, and is dispersed by a double monochromator. A narrow band of the dispersed energy passes through the exit slit and is alternated between reference and sample cells at a rate of sixty cycles per second. These two signals are amplified by the electronics of the photometer and ultimately the ratio of the sample-to-reference signals is presented on a strip-chart record. This ratio gives the transmittance(I/I_o) of the sample. From the Beer-Bouguer Law, the absorption coefficient can be calculated as:

$$\alpha = \frac{1}{d} ln \frac{I_o}{I} \tag{3.1}$$

where d is the sample thickness.

3.2 Results and Discussion

3.2.1 Imidization of Polyimide Films at Various Curing Temperatures

Polyimide films used in this work were formed by imidization of Du Pont PI2545 PMDA-ODA polyamic acid as shown in Fig.3.2. This heat treatment process is called imidization because of the formation of the new imide group(N-CO-) in polyimide. The IR spectra of the polyimide films can be recorded to evaluate the changes of the chemical structure during the imidization.[43,44]

Figure 3.3 shows the IR transmittance spectra of PI samples a and sample d cured at 135 ^{o}C and 350 ^{o}C. The absorption bands for sample a are located at 1310, 1540 and 1654 cm^{-1} which are mainly due to the amino groups(-NH-CO-). These absorption bands do not appear in sample d, but instead, four absorption bands at 723, 1377,1720 and 1778 cm^{-1} corresponding to the absorption of the imide group (N-CO-) appear. These four absorption bands remain unaltered even the samples were further cured at temperatures higher than 350 ^{o}C, indicating that imidization has been completed in sample d cured at 350 ^{o}C. The 1778 and 1720 cm^{-1} bands are commonly attributed, respectively, to the symmetric and asymmetric stretches of the carbonyl groups coupled through the five-membered ring. The band at 1377 cm^{-1} has been attributed

to the C-N stretch. The absorption in the 730 cm^{-1} region has been attributed to deformation of the imide ring or to the imide carbon group.[45] However, both sample a and sample d exhibit an constant absorption band at 1500 cm^{-1} due to the ring breathing modes of the aromatic moieties (C_6H_5-). This band was used as the internal standard for the determination of the degree of imidization. The reproducibility of the imide/internal standard ratio was generally high, with different measurements of the same sample or measurements on duplicate samples. Therefore, we used the ratio of the absorption peak at 1778 cm^{-1} to the absorption peak at 1500 cm^{-1} normalized to the same ratio for sample d as the degree of imidization in percentage.

Figure 3.4 gives the degree of imidization calculated from the IR spectra for polyimide samples at different curing temperatures. The degree of imidization is strongly dependent on the curing temperature between 135 ^oC and 250 ^oC. Since both the chemical and physical structures of the PMDA-ODA polyimide are changed with the imidization, we expect its optical and electrical properties will also be changed. In the following sections, we will study the relations between ultraviolet(UV) absorption and molecular structure of PMDA-ODA polyimide at different curing stage.

3.2.2 Effects of Imide Rings on the Absorption Spectra

The ultraviolet absorption spectra for PI samples a, b, c, and d are shown in Fig.3.5. There are clearly three peaks located at 4.35 eV, 5.65 eV, 6.40 eV and one absorption shoulder at 3.65 eV in the spectrum of the fully cured sample d. These optical transitions may take place within one single molecular chain(intramolecular transitions) or between different molecular chains(intermolecular transitions). The thermal curing has two major effects on the molecular structure of polyimide: One is to promote the formation of imide rings in the chemical structure(imidization) and another is to cause a change of the molecular orders and free volumes between different molecular chains.[46] The formation of imide rings introduces new electron states, thus giving rise to the appearance of the new absorption peaks in the absorption spectra. The absorption coefficient for the polyimide can be expressed in terms of imide rings as

$$\alpha_{imide} = \alpha_o NM \tag{3.2}$$

where α_o is the absorption coefficient per molecule with imide rings, N is the concentration of molecules(including PI and PAA molecules) and M is the degree of imidization. If the first effect or Eq.(3.2) prevails, the four absorption peaks of samples a, b, c, and d should follow the degree of imidization-curing temperature curve. However,

Figure 3.6 shows that none of the four peaks follows the variation of the degree of imidization with curing temperature, each peak value being normalized to its corresponding peak value for the fully cured sample(sample d). This implies that the formation of imide rings is not the major cause for the variation of the absorption peak with curing temperature.

3.2.3 Effects of Charge-Transfer Complexes on the Absorption Spectra

The charge-transfer complexes are formed by the weak interaction of electron donors with electron acceptors. Electron donors are usually π-electronic systems with electron-repelling groups, such as amino, aklkylamino, alkoxy, acetoxy, and alkyl groups. Electron acceptors are usually π-electronic systems with electron-attracting groups, such as nitro, cyano, carbalkoxy, acetyl, carboxylic acid anhydride, and halogen groups. Generally charge-transfer forces do not provide the major contribution to the binding forces in the ground state. Relatively weak interactions between an electron donor(D) and an electron acceptor(A) can be described in terms of a wave function of the form:

$$\Phi_n(AD) = a\Phi_o(A, D) + b\Phi_1(A^- - D^+) \tag{3.3}$$

The wave function Φ_o has been termed the "no bond" function. It corresponds to the structure in the complex in which binding results from such "physical" forces as dipole–induced-dipole interactions. The wave function Φ_1 has been termed the "dative" function. This corresponds to a structure of the complex where one electron has been completely transferred from the donor to the acceptor. The electronic absorption extra to the absorption of the components is often observed when charge-transfer complex is formed. For weak interaction the transition is effectively from the structure $\Phi_o(A, D)$ to the structure $\Phi_1(A^- - D^+)$. The energy of the charge-transfer transition E_{CT} is related to the ionization potential of the donor I_D and the electron affinity of the acceptor E_A as:

$$E_{CT} = I_D - E_A - W \tag{3.4}$$

Where W is the dissociation energy of the charge-transfer excited state.

PMDA-ODA polyimide falls into the class of electron donor-acceptor polymers, by virtue of the diphenlether and the pyromellitimide groups in the polyimide. The formation of charge transfer(CT) complex can be indicated by CT bands in the absorption spectra. From Fig.3.5, The absorption peak p_4 at 6.40 eV in the fully cured sample (sample d) also appears in the non-fully cured samples(samples a, b, and c), but it becomes broader and occurs at

a lower energy in samples a and b. The absorption peak p_4 at 6.40 eV in the fully cured PMDA-ODA polyimide has been suggested[20] to be due to π-π^* intramolecular transitions. The absorption peak consists of a strong π-π^* transition as its major component surrounded by other weaker π-π^* transitions. Samples c and d basicly consist of polyimide only. Samples with lower degree of imidization such as samples a and b, are actually the mixture of polyimide and its precursor PAA. The XPS and SXPS spectra have shown[18] that the π states in polyimide are different from those in PAA. The shift of the peak position from 6.40 eV for sample d to 6.27 eV for sample a and the broadering of the absorption peaks for samples a and b reflect the changes of such π states during cure.

Comparing with absorption peak p_4 which is relatively insensitive to the changes of curing temperature, the behavior of absorption peak p_3 at 5.65 eV is quite different. It appears as a clear absorption peak in samples d and c and degenerates to an absorption shoulder in sample b and gradually disappears in sample a. It should be noted that sample d and sample c have almost the same degree of imidization, which means that their molecular chemical structures are basicly the same. This leads us to think that the changes of the absorption peak at 5.65 eV are propably due to changes of interactions between different molecular chains during cure. The

formation of intermolecular charge-transfer complexes in polyimide has been experimentally confirmed.[47] The higher absorption peak in the fully cured sample d is due to stronger intermolecular transitions between polyimide chains. Figure 4.7 compares our mearsured absorption spectrum of sample d with the computed absorption spectrum of PMDA-ODA polyimide.[18] The obvious difference between two spectra is that the peak at 5.65eV seems to be missing from the computed spectrum. In this computation the polyimide is assumed to be constituted of PMDA-ODA unit cells for which the electronic states are highly localized and the interactions between different molecular chains can be neglected. In other words, the computed spectrum does not include any intermolecular effects. The dispency between the measured spectrum and the computed spectrum at 5.65eV indicates that the absorption peak around 5.65 eV is due to the formation of charge transfer complex between the different chains.

Absorption peak p_2(at 4.35 eV) also increases with the increasing curing temperature. Unlike absorption peak p_3(at 5.65 eV), the absorption peak p_2 does appear in the computed PMDA-ODA polyimide absorption spectrum in which only intramolecular transitions are expected. As has been mentioned above, the changes of the chemical molecular structure due to the formation of imide

rings are not expected to be responsible for such absorption changes during cure. Several investigators have reported that the degree of ordering in the polyimide films changes as imidization proceeds.[48,49] The X-ray diffraction analysis has shown that the polyimide films change from a totally amorphous to a partially crystalline stracture as the curing temperature increases[50], and that there are differences in the degree of anisotropy for the polyimide films at different stages in the cure. The IR absorption spectrum of polyimide has been found to depend on the degree of anisotropy which varies with curing temperature. It is therefore likely that morphological changes in the polyimide films during cure could lead to the appearance of different absorption peaks in the visible-UV spectra. The small absorption shoulder p_1(at 3.65 eV) only appears in sample d. Since the major difference between sample c and sample d is the change in the degree of intermolecular ordering, it is likely that the absorption shoulder p_1 in sample d is due to intermolecular charge transfer between chains.

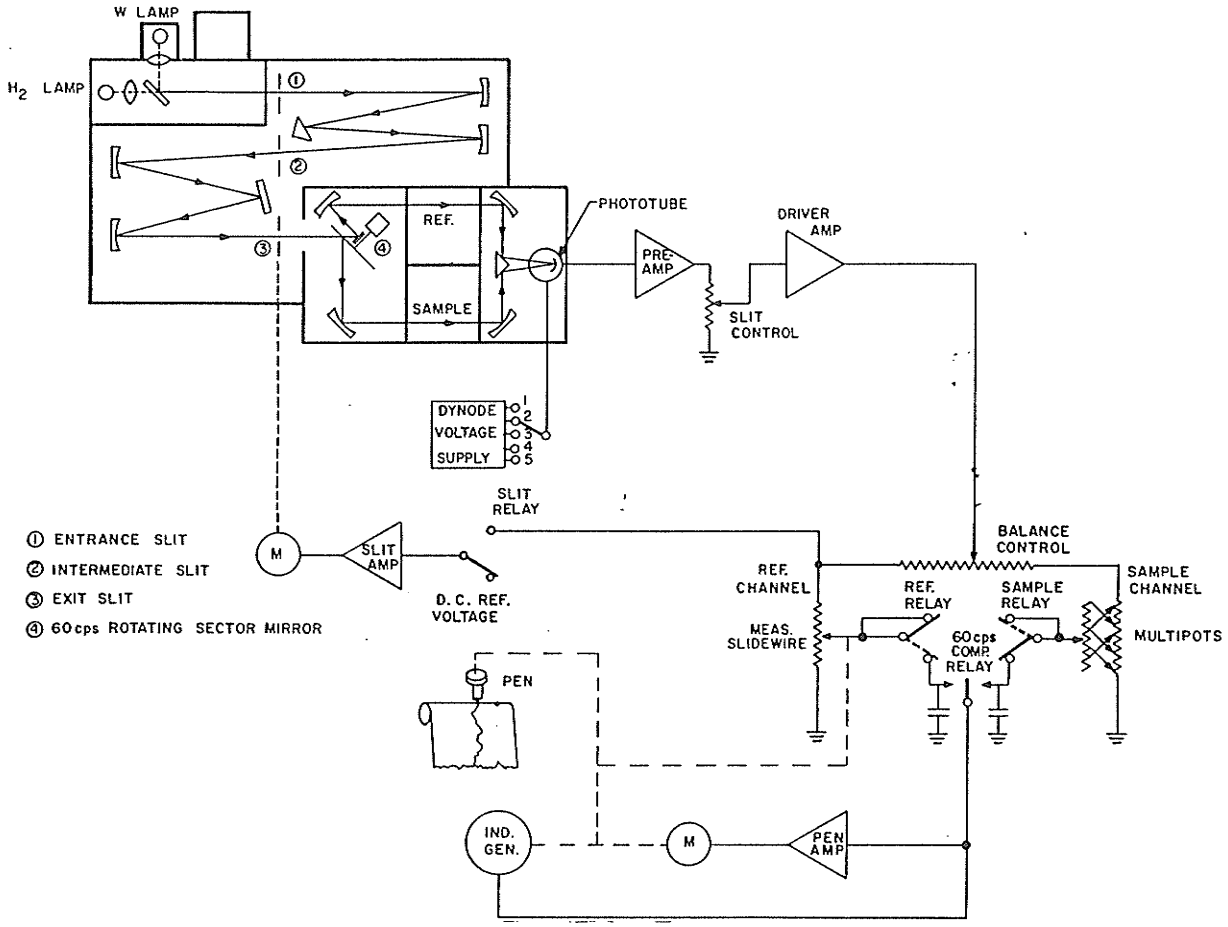

Figure 3.1: The simplified diagram of the optical and photometric system of Cary 14 spectrophotometer.

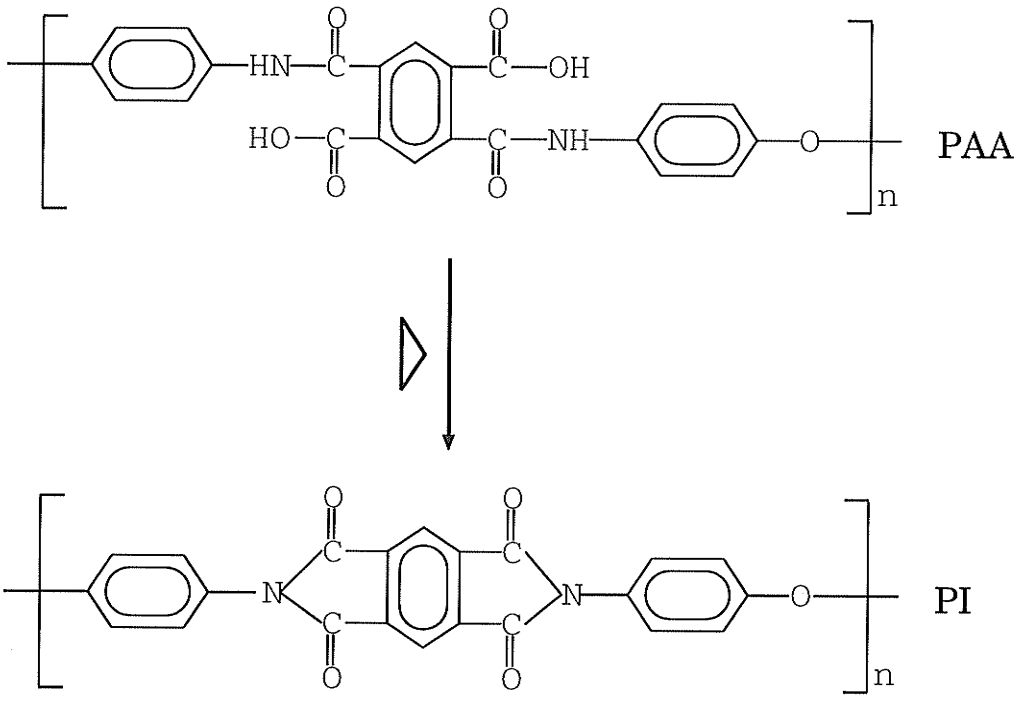

Figure 3.2: Imidization reaction of the polyimide.

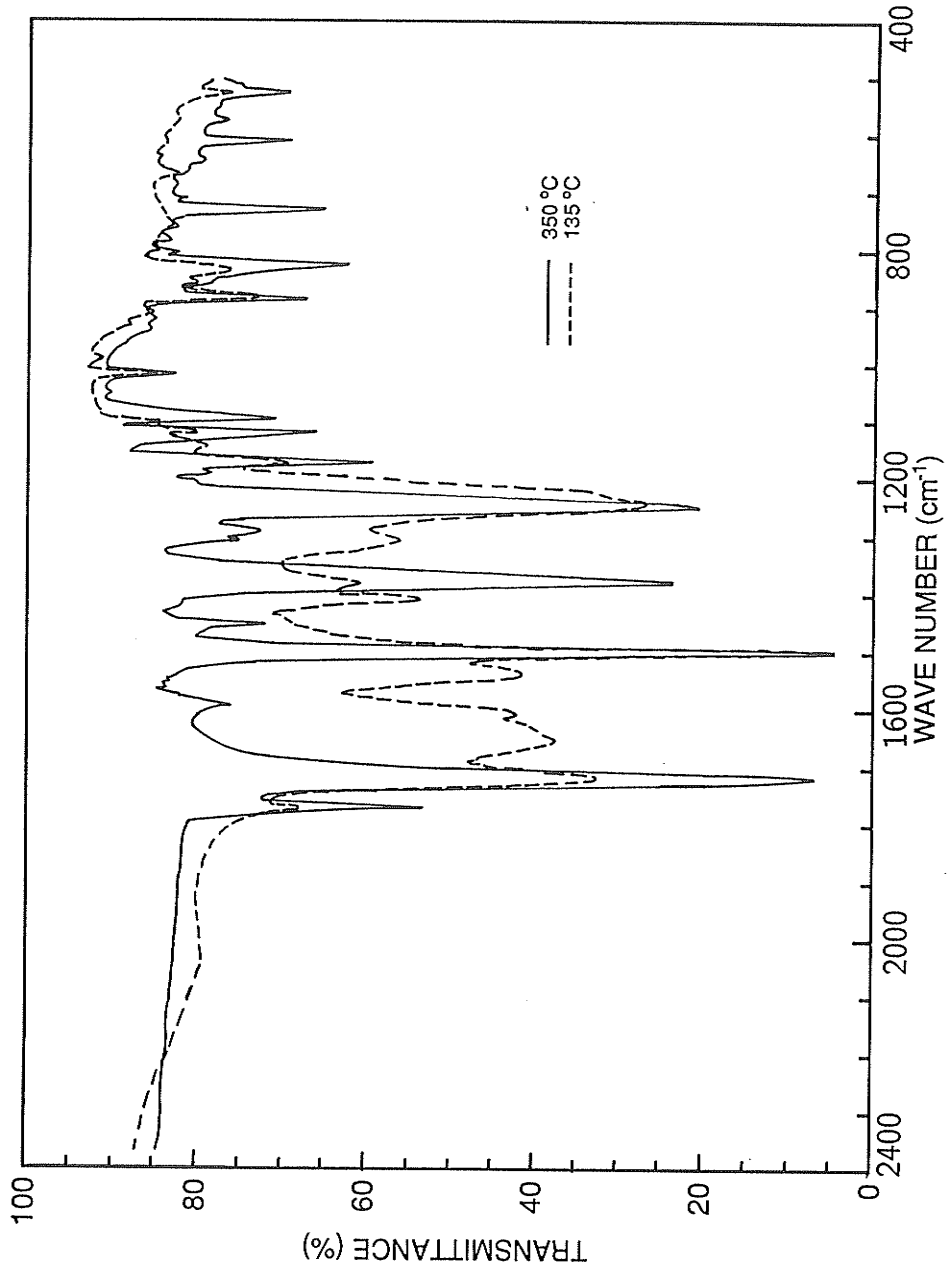

Figure 3.3: IR transmittance spectra of PI samples a and sample d cured at 135 °C and 350 °C.

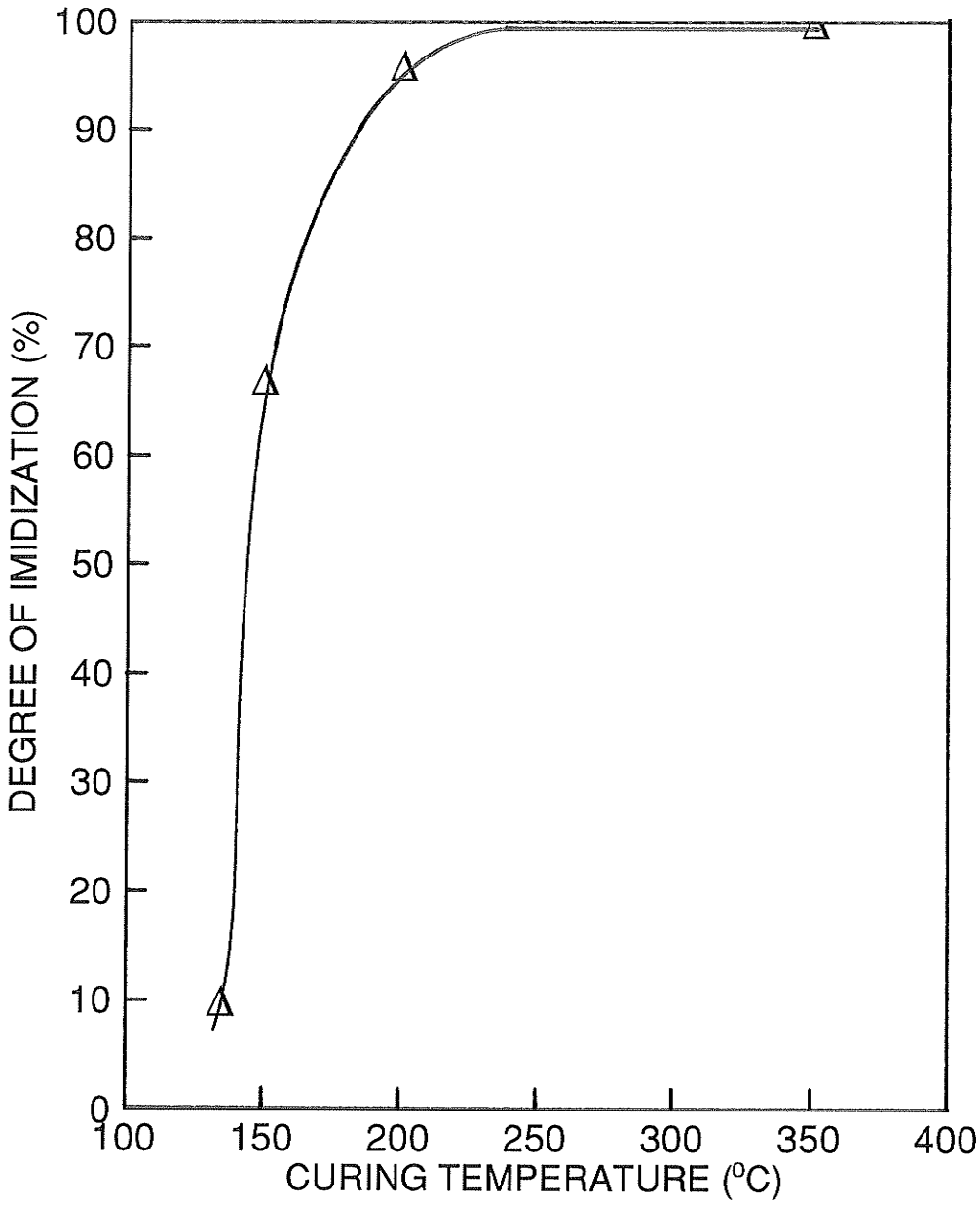

Figure 3.4: Degree of imidization of polyimide samples at different curing temperatures

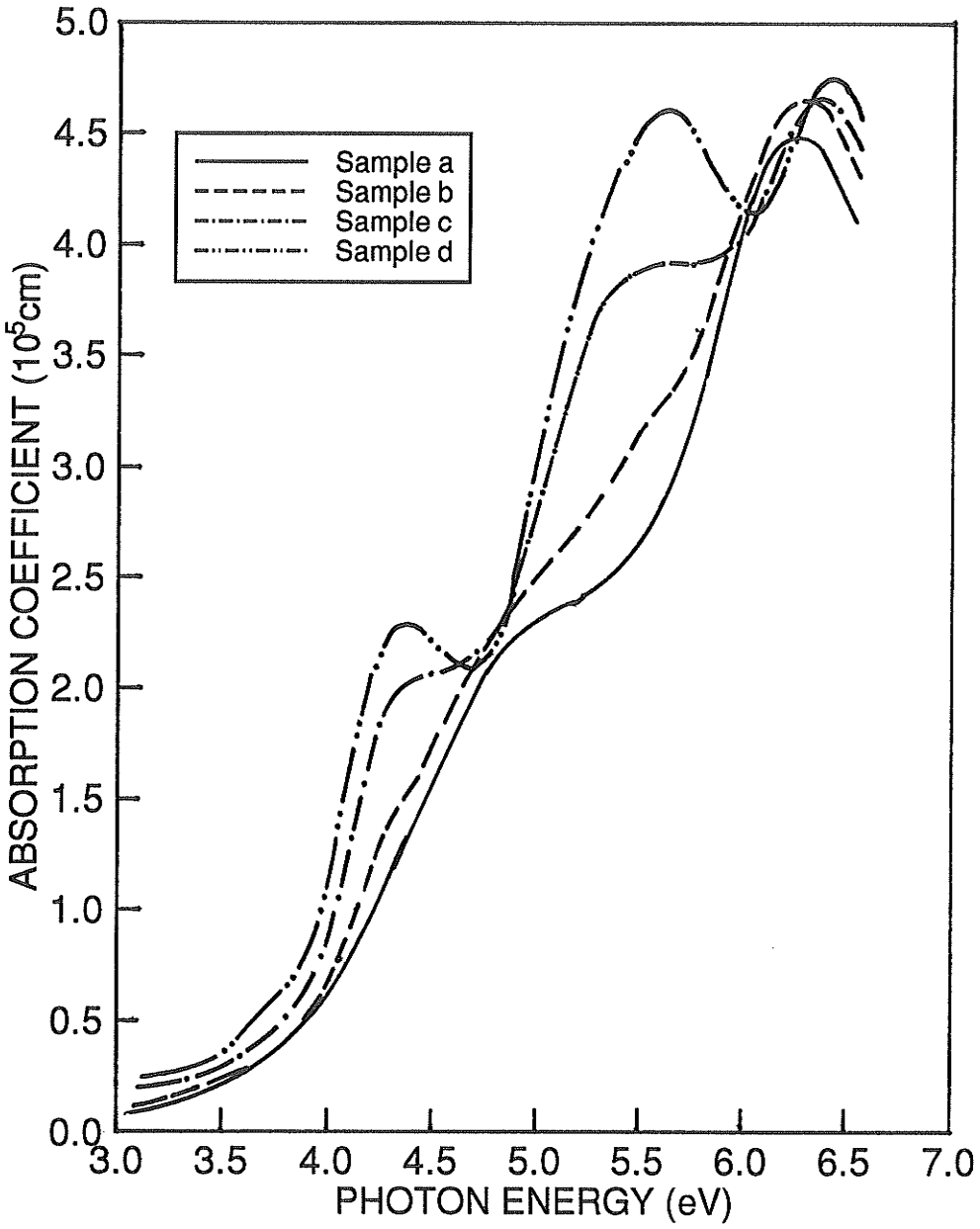

Figure 3.5: Absorption spectra of PI samples a,b,c,d with sample thicknesses ranging from 0.60 to 0.78 μm.

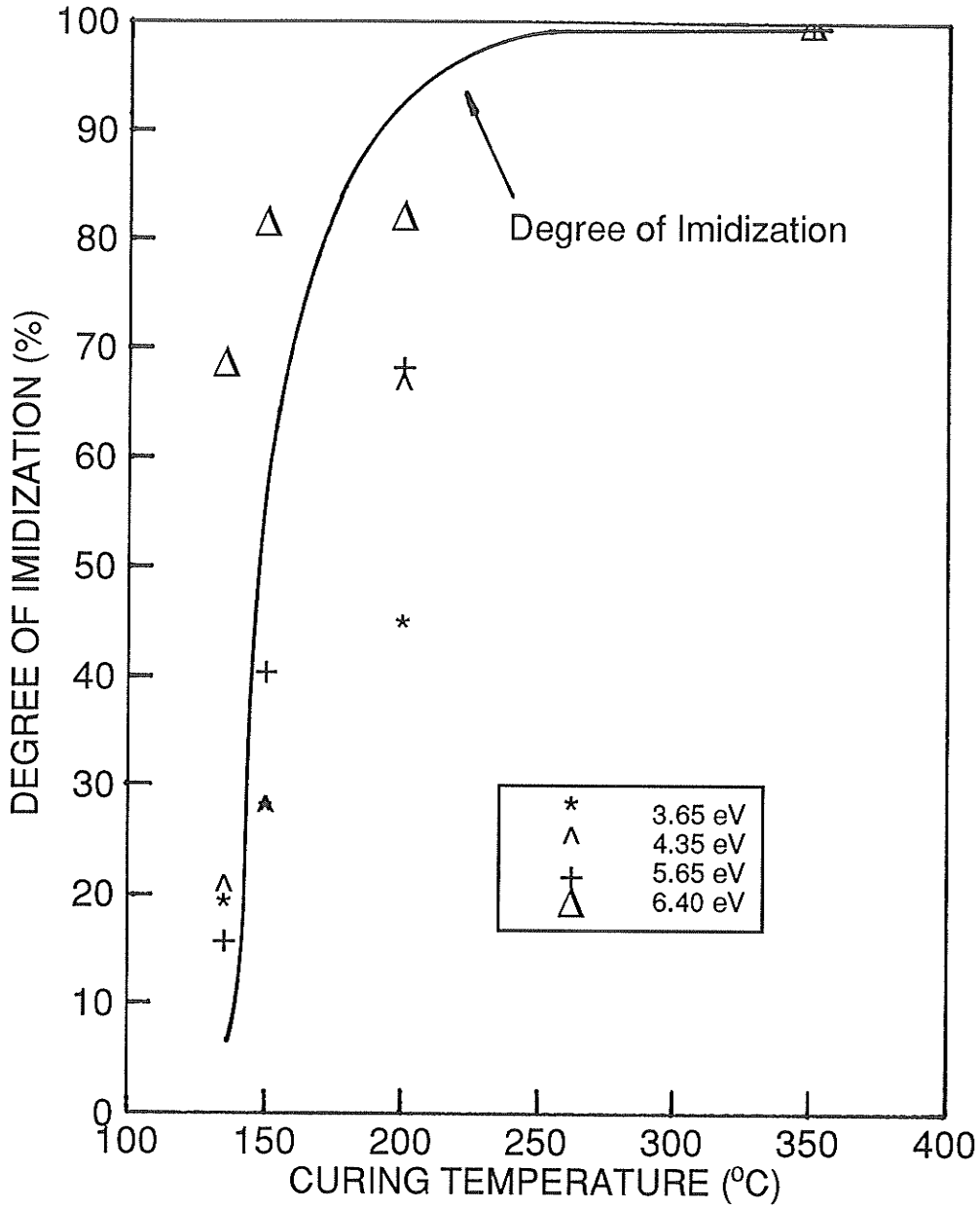

Figure 3.6: The degree of imidization and the normalized absorption peaks of samples a,b,c and d as functions of curing temperature. The absorption peaks are normalized to the peaks of sample d which is considered to have 100% in degree of imidization.

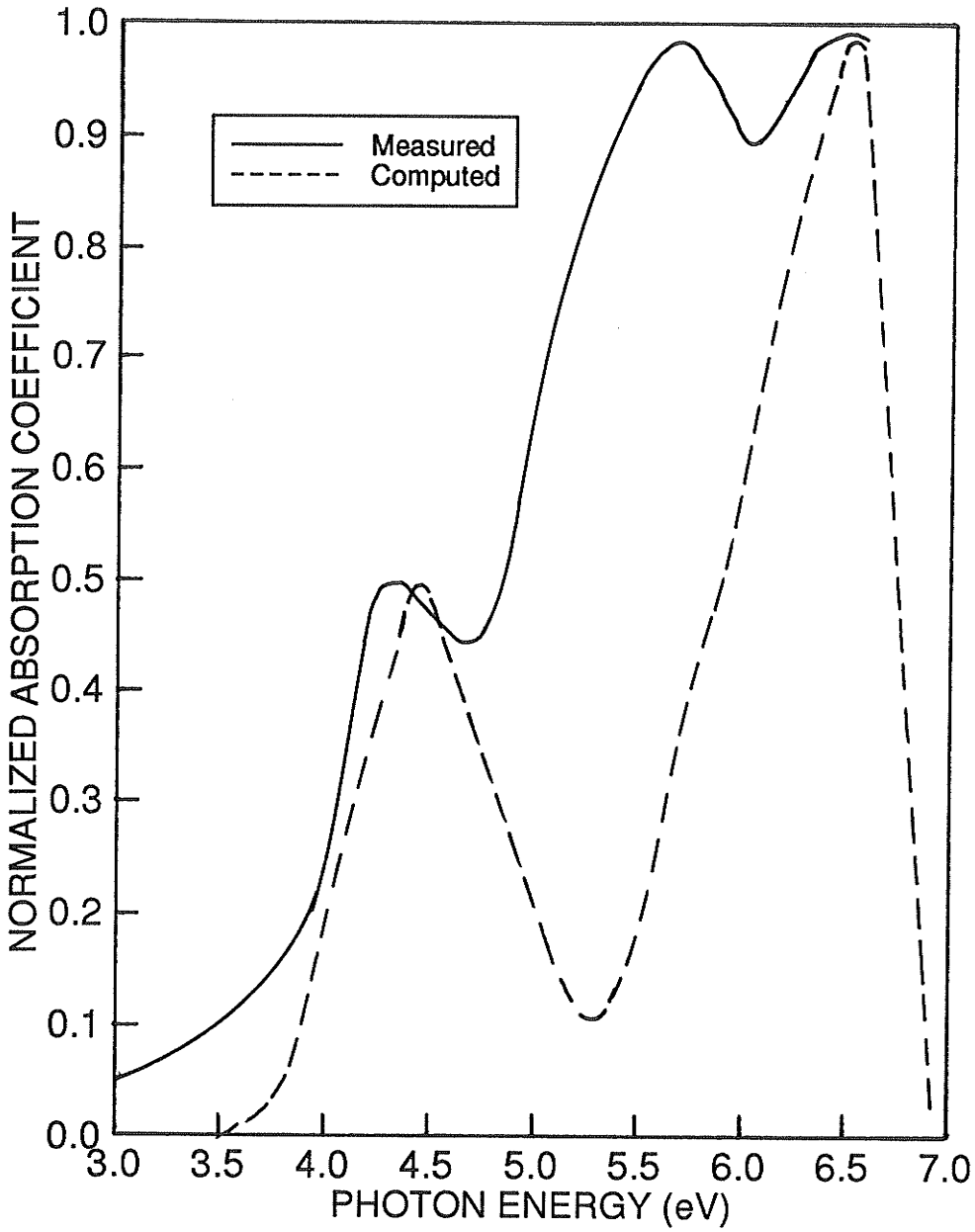

Figure 3.7: The measured absorption spectrum and the computed absorption spectrum of fully cured PMDA-ODA polyimide.

Chapter 4

Ultraviolet Photocurrent Spectra of PMDA-ODA Polyimide Films at Various Curing Temperatures

Photoconduction measurement has been widely used as a method for the study of the electrical conduction processes in highly insulating materials such as polyimide because photoexcitation can generate a large quantity of charge carriers which make the current measurement much more accurate. Experimental and theoretical studies on the electrical properties of polymers and their complexes have been carried out intensively in the past decades.[51–53] There are two fundamental processes in the photoconduction phenomena: the first is the generation of charge carries and the second is their transport. It is known that the formation of charge complexes is crucial for the carrier generation processes. Information about this can be obtained by measurements of either the photocurrent spectra or the electrical field dependence of the photocurrents.

Photoconduction in the visible region has been reported to be independent of the material and the applied voltage polarity of the illuminated electrode.[19,42] However, in the ultraviolet region we have observed the dependence of both the material and the applied voltage polarity in polyimide.[41] Many mechanisms for charge carrier generation by light in polymers have been reported. Of the important ones are the production of electron-hole pairs in the bulk and the injection of both carriers from the electrodes. In this chapter, we shall present the results of the photocurrent spectra of PMDA-ODA polyimide at various curing temperatures in the UV region and the field dependence of the photogeneration quantum efficiency. The results have been analysed using Frenkel and Onsager theories. A simple model to provide a qualitative description about the photogeneration processes in polyimide is given.

4.1 Experimental Techniques

For photocurrent measurements the substrates used were $< 100 >$ oriented, n-type, 1-2 Ω-cm silicon wafers which had already been vacuum-deposited with a thick aluminum layer as the bottom electrode. A gold or silver layer of thickness of 100 $\AA$ was deposited on the PI film surface as the top illuminated electrode. The thickness of this illuminated electrode was controlled by a TM-100 film thickness

monitor during deposition to ensure its thinness. However, a small thick aluminum dot of about 2000 $\AA$ was also vacuum deposited on the thin illuminated electrode surface to ensure a good electrical contact, the area of the electrode surface and the dot being 10 mm^2 and 2 mm^2, respectively. Table 4.1 summarizes the parameters of the typical polyimide samples used for photocurrent measurements.

Table 4.1 The typical PI samples used for photocurrent measurement

Sample	Thickness(μm)	Curing Temperature(^{o}C)	Imidization(%)
A	1.55	135	10
B	1.43	150	67
C	1.32	200	96
D	1.20	350	100

The experimental arrangement for photocurrent measurements is shown in Fig.4.1. The light source was a 150 W xenon lamp for photon energies from 3.0 eV to 3.7 eV and a 50 W deuterium lamp for photon energies from 3.7 eV to 6.5 eV. The lamp was mounted in a housing with sphercial mirror, lens and slit to provide a paralled beam which is guided to pass through a HR-320 monochromator and focused through a set of UV quaze lens onto the sample. The beam size was 4.0 mm^2 in area which was smaller than the size of top illuminated electrode. The scanning speed of the monochromator was set to 35 $\AA$/sec with a grating of 1200 g/mm. The incident light spectra were measured using an Optikon 550-1 photometer in con-

junction with an EMI 9588QB photomultiplier. The photocurrent was measured using a Keithley 610C electrometer in conjunction with a HP-7132A strip recorder. Blank test of the sample holder inside the chamber showed a stray current less than 10^{-14} A with and without light ilumination, which was two to four orders smaller than the measured photocurrents. All the measurements were performed in a vaccum chamber of 5×10^{-6} torr at room temperature (22 ^{o}C).

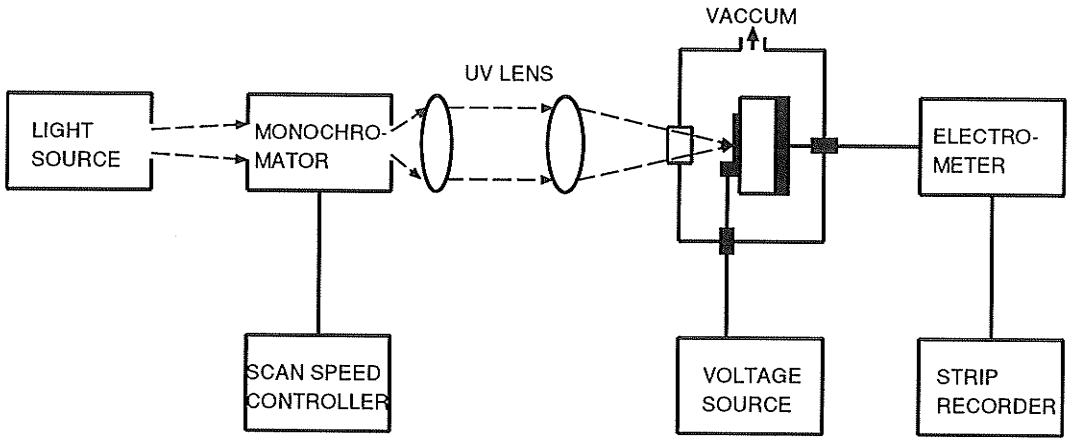

Figure 4.1: Experimental arrangement for photocurrent measurements.

The photocurrent spectra were measured after the dark currents have reached their steady states. For the measurement of photocurrent as a function of applied electric field, the chopped UV light pulse with duration of 5 seconds were used because of large transient dark current after the DC voltage was applied. The pho-

tocurrent was measured after the application of voltage for 20 seconds. It is important to ensure that all the samples are under same condition before each individual measurement. Since for polymer with high resistivity like polyimide it usually takes days to allow the sample entirely back to its original state after each measurement, we set up a preliminary conditioning process in which after each measurement the sample was short-circuited and illuminated under UV light for 10 minutes and then rested in the dark for 5 minutes before making another measurement. Under such condition the dark and illuminated short-circuit currents are negnigible compared with the measured photocurrents.

4.2 Results and Discussion

4.2.1 Quantum Efficiency Spectra

Photoconduction quantum efficiency Φ is defined as the ratio of the number of charge carriers producing photocurrent generated by photoexcitations to the number of photons absorbed by the material during the same period of time, and it can be expressed as

$$\Phi = J_{ph}/qI_0T \tag{4.1}$$

where J_{ph} is the photocurrent density, I_o is the number of incident photons per unit area per second, and T is the transmittance of

the illumilated electrode. Figure 4.2 shows the spectra of normalized intensities of the incident light from the Xenon lamp and the Deterum lamp. Figure 4.3 shows the quantum efficiency spectra of fully cured polyimide sample D with different polarities and materials at the illuminated electrode. There are clearly four peaks which are not located at the same photon energy as those in the absorption spectra in Fig.3.5, but rather, at 3.55 eV, 4.05 eV, 4.90 eV and 5.80 eV. In the previouse studies, only photocurrent peak at 3.55 eV was reported.[19,54] In order to observe quantum efficient peaks at 4.05 eV, 4.9 eV and 5.80 eV, it is important to chose the appropriate light source. Xenon lamp which was mostly used in photocurrent measurement of polyimide was found not good to obtain these quantum efficiency peaks, because Xenon lamp produces a large photocurrent peak around 3.55 eV which will overlay the much smaller photocurrent peaks produced by the much weaker incident light above 3.55 eV. On the other hand, Deterum lamp gives the relative strong incident light in UV region (4.0 eV-6.0 eV) comparing with the incident light in visible region(<4.0 eV) and can be used as a light source to produce the photocurrent of polyimide in UV region. Figure 4.3 also shows the quantum efficiency spectra depend on the polarity and the material of the illuminated electrode. It can be seen that for the case with the illuminated electrode at the negative polarity the

spectra are strongly dependent on the electrode material for photon energies higher than 4.4 eV. For the case with the illuminated electrode at the positive polarity, such polarity dependence is much smaller, and also the quantum efficiency is smaller for photon energies higher than 3.75 eV. These results indicate that photoemission of electrons from the negative illuminated electrode plays a dominant role in photoconduction for photon energies higher than 4.4 eV. By assuming that the carriers injected from the illuminated electrode due to photoemission and mainly electrons, then $(\Phi)^-_{Au}-(\Phi)^+_{Au}$ and $(\Phi)^-_{Ag}-(\Phi)^+_{Ag}$ can be considered as the quantum efficiency contributed by photoemission, and $(\Phi)^+_{Au}$ or $(\Phi)^+_{Ag}$ contributed mainly by photoexcitation in the bulk. According to Fowler equation for photoemission from a metallic electrode to an insulator, the quantum yield due to photoemission is proportional to $(h\nu\text{-}\phi)^2$, where $h\nu$ is the photon energy and ϕ is the threshold barrier height. The plot of $[(\Phi)^-_{Au}-(\Phi)^+_{Au}]^{1/2}$ and $[(\Phi)^-_{Ag}-(\Phi)^+_{Ag}]^{1/2}$ as functions of $h\nu$ is shown in Fig.4.4. The extrapolation of the plot to the zero quantum yield abscissa in Fig.4.4 gives ϕ of 4.17 eV for the Au and of 4.37 eV for the Ag illuminated electrode. These barrier heights are not determined by the work function differences between metals and polyimide as found for photoemissions in most polymers[55] due to the presence of the metal-polymer interface states.

For positive polarity the quantum efficiency is independent of the material of the illuminated electrode as shown in Fig.4.3. A similar finding has been repored [19,44] for thick polyimide film of 25 μm at a photon energy of 3.55 eV. Figure 4.5 shows the quantum efficiency spectra of polyimide samples with different curing temperatures under positive illuminated electrode. The relationship between the quantum efficiency and the curing temperature is similar to that for the absorption peaks shown in Fig.3.5. For example, the absorption peak p_3(at 5.65 eV) is missing in samples a and b, so is the quantum efficiency peak P_3(at 4.90 eV) in samples A and B. Quantum efficiency peak P_4(at 5.80 eV) as well as its corresponding absorption peak p_4(at 6.40 eV) appears in all four samples with different curing temperatures. The correspondences between the quantum efficiency peaks and the absorption peaks indicate that the photoconduction carriers are mainly generated in the bulk. Figure 4.6 compares the quantum efficiency spectrum with absorption spectrum of fully cured polyimide samples D and d. The quantum efficiency peaks shift to the lower energy from the corresponding absorption peaks. A similar phenomenon has also been reported in anthracene in which photocurrent is generated by a single photon intrinsic process.[56] It is well known that in contrast with the extrinsic photoconduction for which the action spectrum is simi-

lar in shape to the absorption spectrum, there is no direct relation between the intrinsic photocurrent and the absorption spectrum.[57]

The energy gap of polyimide is about 7 eV[17], the possibility of photogeneration due to band-to-band transition via a single-photon process can be ruled out for the range of photon energies used in this investigation. Thus, the photogeneration of carriers responsible for the photocurrent is due to a carrier generation process via metastable states. Freilich has reported[1] that the incorperation of electron donors to PMDA-ODA polyimide results in an enhancement of photocurrent in the visible region due to the formation of the charge-transfer(CT) complexes between the doped donors and the pyromellitimide(acceptors). PMDA-ODA polyimide has a unique molecular structure in which the diphenlether group acts as donors and the pyromellitimide group acts as acceptors, and they form donor-acceptor pairs.[58] Optical illumination causes transfer of electrons from the donors to the acceptors resulting in the formation of the positive and the negative charge pairs. The dissociation of these pairs gives rise to photocurrent. The photocarrier generated rate of such a process will depend on the applied electric field and the thermal stress. Several investigators have reported the field dependence of the photogeneration quantum yield for polymers, such as PVK[59] and PVK/TNF[60–62]. In the following section, we will

discuss the field dependence of the quantum efficiency of polyimide.

4.2.2 Field Dependence of the Quantum Efficiency

Photogenerations in polyimide have been described due to formation of charge-transfer(CT) complexes between donors and acceptors. Under the applied electric field, the opposite charges will escape their mutural Coulomb attraction and transport via hopping between donor or acceptor sites. There are two similar theories proposed by Frenkel[63] and Onsager[64] which have been generally used to analyse such photogeneration processes. In both cases the electric field dependence of photogeneration quantum yield arise from a reduction of the ionization energy for the seperation of two charges under their mautual Coulomb attraction. The resulting dependence of photogeneration quantum yields on electric fields using this two treatments are substantially different. In the following we will analyse our experimental results based on the Frenkel and Onsager formulation, respectively.

Frenkel's analysis of the electric-field-assisted thermal ionization of charge carriers is based on a physical model in which an electron under the Coulombic influence of a fixed positive charge embedded in a uniform dielectric medium. In the absence of applied electric field, the propabilities of the electron escaping the potential barrier

E_o because of thermal excitation are same in all the directions and the net current will be zero. In the presence of the applied electric field, the barrier height will be lowed by ΔE_o alone the electric field

$$E_b = E_o - \Delta E_o = E_o - \beta E^{1/2} \tag{4.2}$$

where $\beta = (e^3/\pi\epsilon_o\epsilon_r)^{1/2}$, ϵ_o and ϵ_r are the dielectric constant of vaccum and the relative dielectric constant of the medium, respectively. The probability of the electron escape in the presence of a electric field is proportional to exp[($\beta E^{1/2}$-E_o)/kT]. Thus the logarithm of the quantum efficiency is expected to vary linearly with the square root of electric field. Figure 4.7 shows the plots of lgΦ_{ph}(E) versus $E^{1/2}$ at photon energies 4.05eV, 4.90eV and 5.80eV. None of them is a straight line. We therefore turn our attention to the Onsager model.

The Onsager theory has been succesfully applied to the photogeneration of free carriers in solids, espicially in PVK[59], amorphous selenium[65] and PVK/TNF[60]. This theory is based on the assumption that part of the absorbed photons pruduce bound thermalized elecron-hole pairs which either recombine or dissociate under the combined effects of the Coulomb attraction and the applied electric field. The overall generation efficiency can be expressed as:

$$\Phi(E) = \Phi_o \int p(r_o, \theta, E) g(r, \theta) d^2r \tag{4.3}$$

where Φ_o is the primary quantum yield which is independent of the applied field; p(r,θ,E) is the probability of which the bound pairs with a distance r_o at an angel θ to the applied electric field E can avoid recombination; g(r,θ) is the initial spatial distribution of bound charge pairs. With the assumption that g(r,θ) is an isotropic δ function

$$g(r,\theta) = (4\pi r_o^2)^{-1}\delta(r - r_o) \tag{4.4}$$

A solution of equ.(5.3) has been given as[66]:

$$\Phi(r_o, E) = \Phi_o[1-(-\frac{eEr_o}{kT})^{-1}\sum_{k=0}^{\infty} A_k(\frac{e^2}{4\pi\epsilon_o\epsilon_r kTr_o})A_k(\frac{eEr_o}{kT})] \tag{4.5}$$

where A_k is a recursive formula given as:

$$A_{k+1}(x) = A_k(x) - x^{k+1}exp(-x)/(k+1)! \tag{4.6}$$

with A_o=1-exp(-x). The sum in equ.(4.5) is convergent and can be calculated by increasing k until last term is found which is less than some fraction of the sum to that point. In our computation ϵ_r was taken as 3.5 for polyimide and a test fraction of 10^{-5} was chosen.

Figure 4.8 shows the electric field dependence of the photogeneration efficiency of polyimide sample D measured with the incident photon energy at 4.05 eV, 4.90 eV and 5.80 eV, respectively. The curves in Fig.4.8 were calculated from equ.(4.5) assuming values of the initial thermalization distance r_o at 29, 30 and 31 $\mathring{A}$. The experimental results are in good agreement with those predicted from the

Onsager theory by chosing the different primary yield Φ_o at each photon energy. Figure 4.9 gives the similar results for sample C. The primary yield Φ_o and initial charge distance r_o for samples C, D at different incident photon energies are listed in Table 4.2.

Table 4.2. The primary yield Φ_o and the initial seperation r_o for samples C and D

Photon Energy (eV)	Φ_o		$r_o(\mathring{A})$	
	Sample C	Sample D	Sample C	Sample D
4.05	7.0×10^{-4}	2.1×10^{-3}	30	30
4.90	7.4×10^{-4}	2.4×10^{-3}		
5.80	8.0×10^{-4}	1.5×10^{-3}		

The initial thermalization distance r_o is 30 $\mathring{A}$ which is in good agreement with 30 $\mathring{A}$ and 35 $\mathring{A}$ found in PVK[61] and PVK/TNF[67] in UV region but is larger comparing with 15 $\mathring{A}$ and 13 $\mathring{A}$ reported in polyimide[68] and polyimide/DMA[1] in visible region. The constant r_o for all three different incident photons in samples C and D indicate that the bound electron-hole pairs generated by absorbed photons are same in the UV region no matter these bound electron-hole pairs are intermolecular or intramolecular. Changes of the intermolecular structure during cure do not form the new kind of bound electron-hole pairs. The primary yield Φ_o increases with the curing temperature. As has been mentioned before, the photocurrent peaks at 4.05 eV and 4.90 eV are believed to be associated with

the absorption peaks at 4.35 eV and 5.65 eV which are due to intermolecular transitions. The intermolecular ordering changes from sample C to sample D increase the number of bound electron-hole pairs produced by incident photons and contribute to the increasing primary yield Φ_o as shown in Table 4.2. The quantum yield at 5.80 eV is associated with the absorption peak at 6.40 eV which is due to intramolecular transition. Sample C and sample D have almost same degree of imidization. The intramolecular structures are expected same for both sample C and sample D. However, the experimental results in Table 4.2 show that the primary yield Φ_o at 5.80 eV is larger in sample D than the primary yield in sample C although the increase is less significent comparing with the primary yield increases at 4.05 eV and 4.90 eV. It should be noted that the dark current is smaller in sample D than in sample A. It has been reported that the steady-state dark current in polyimide is predominant by the hole injection from the electrode.[69] These hole carries will combine with the photo-generated electrons and cause the quntum efficiency decresed. The dependence of photocurrent on dark current has also been observed in polyethylene.[70] Furthermore polyimide is not a ideal trap-free material. The intermolecular structure changes during cure may change the precence of traps in the material which will affect the quantum yield. Considering

the above experimental results, a simple model accounting for the photocarrier generations in PMDA-ODA polyimide is proposed as follows: irradiation of donor-acceptor pairs (the diphenlether and the pyromellitimide) makes electron transfer from the donor to the acceptor resulting in formation of the positive and negative charge pairs. Because of the low mobility and short mean free path, the optical excited carrires will be easily trapped by the columbic field of these charged centers and form the metastable states. Both intramolecular and intermolecular charge complexes are formed under the UV irradiation and they are same in nature. The excess photon energies will be either lost through non-radiative decay or used to seperate these electron-hole pairs under assistances of the applied electric field and the thermal stress. The dissociation of the electron-hole pairs will give the photocurrent.

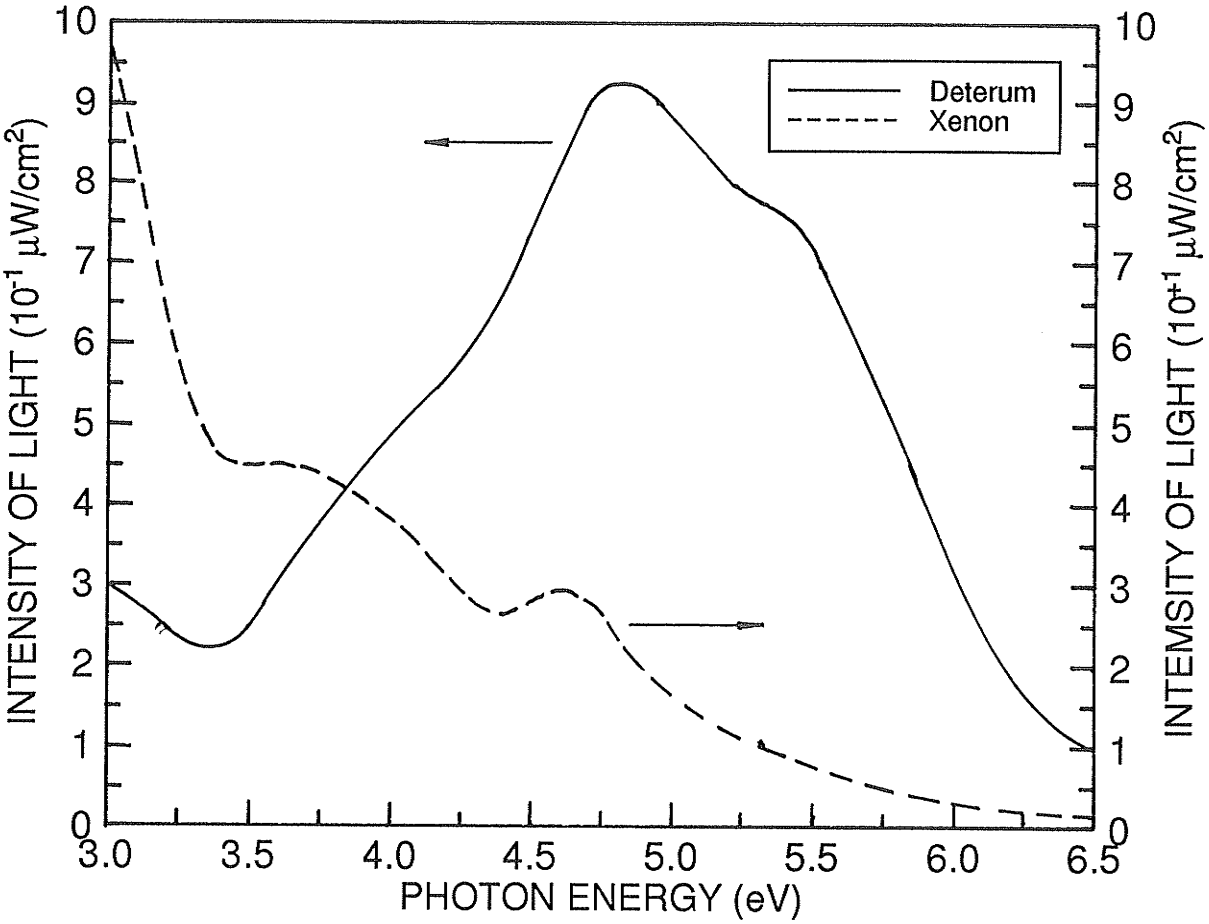

Figure 4.2: Spectra of the incident light from the Deterum lamp and the Xenon lamp.

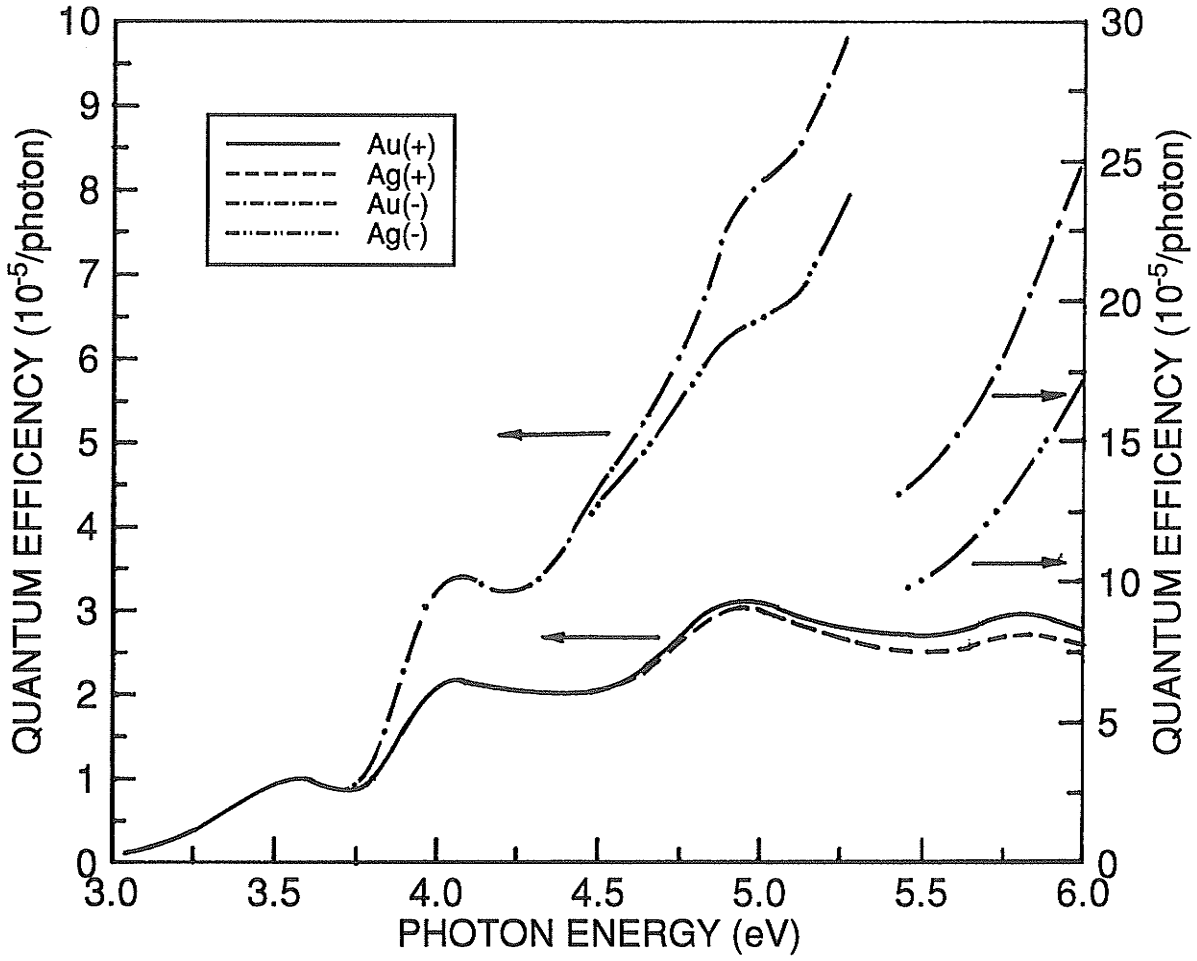

Figure 4.3: Quantum efficiency spectra of fully cured polyimide(sample D) for the illuminated electrode at the positive or the negative polarity at an applied field of 1.17×10^5 V/cm.

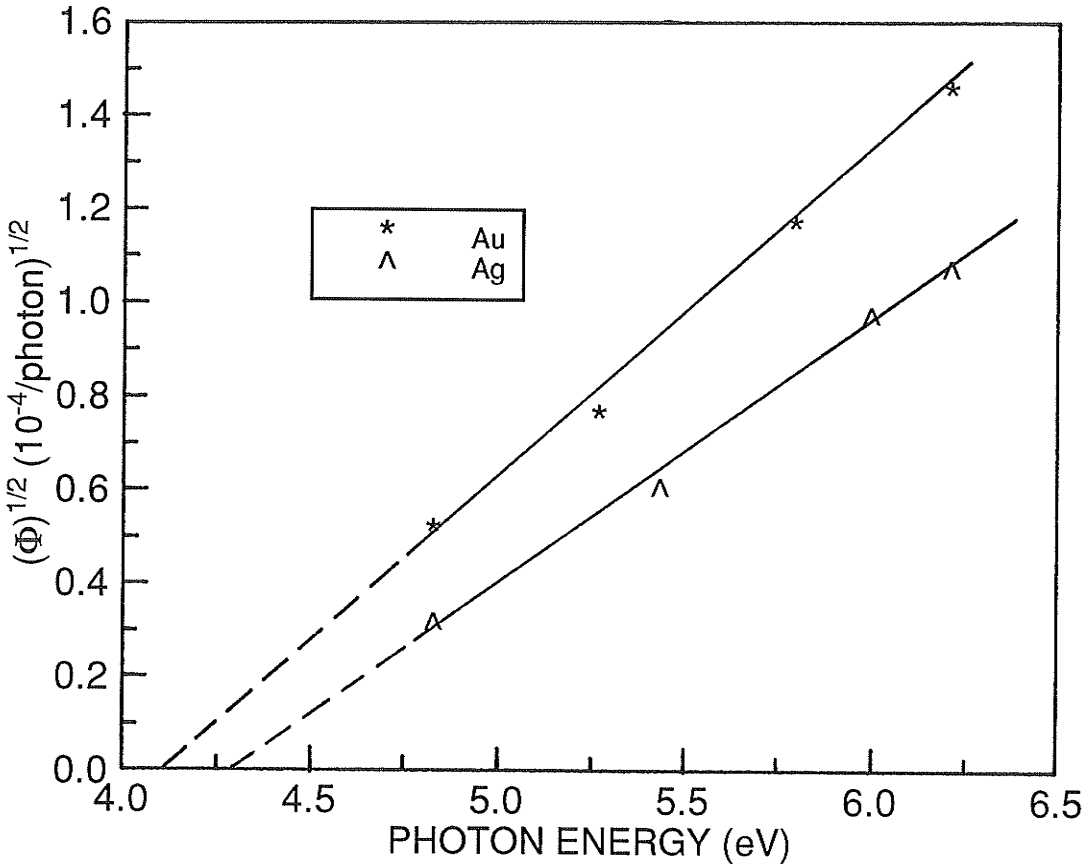

Figure 4.4: Plot of $(\Phi)^{1/2}$ as a function of photon energy for the case with the illuminated electrode at negative polarity. Applied field 3.33×10^4 V/cm

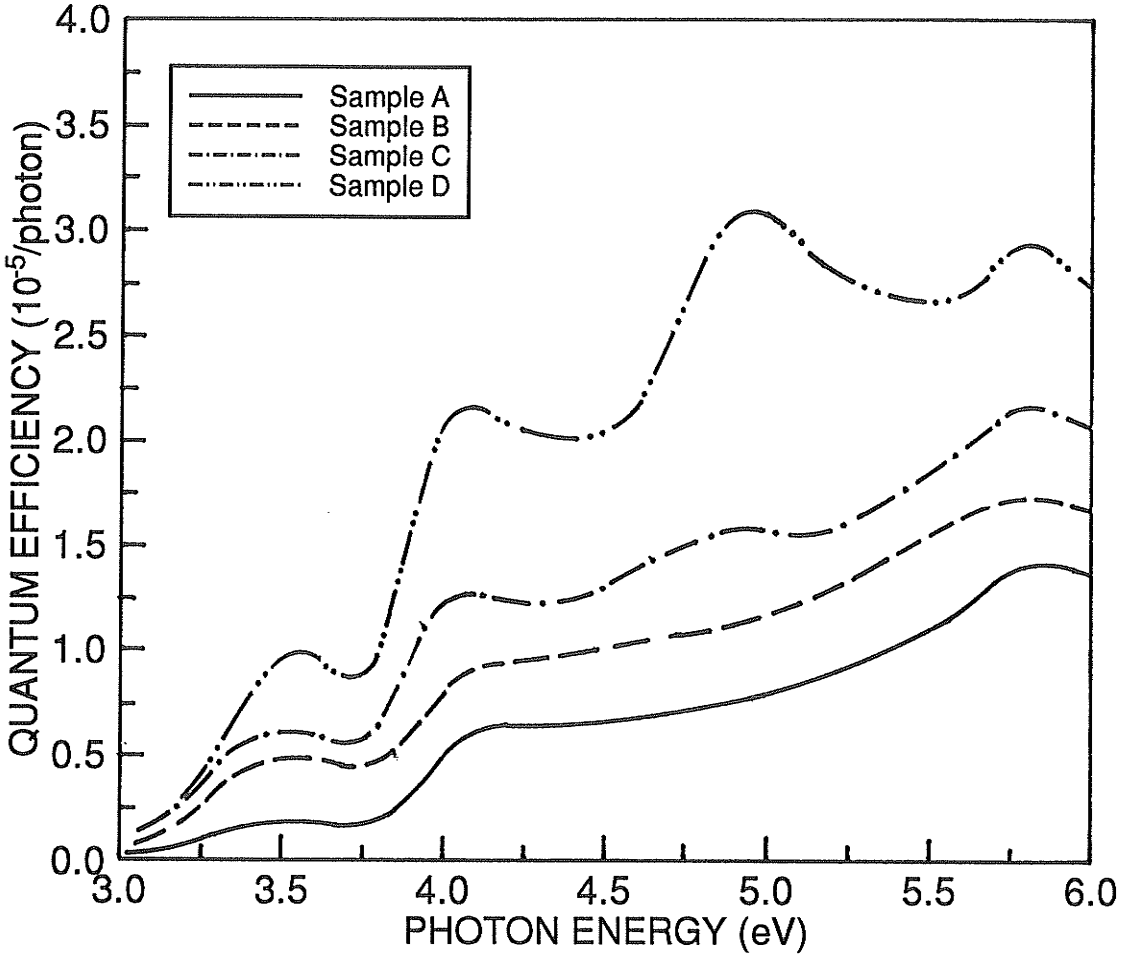

Figure 4.5: Quantum efficiency spectra of samples A, B, C and D for the illuminated electrode at the positive polarity and the applied field of 1.17×10^5 V/cm.

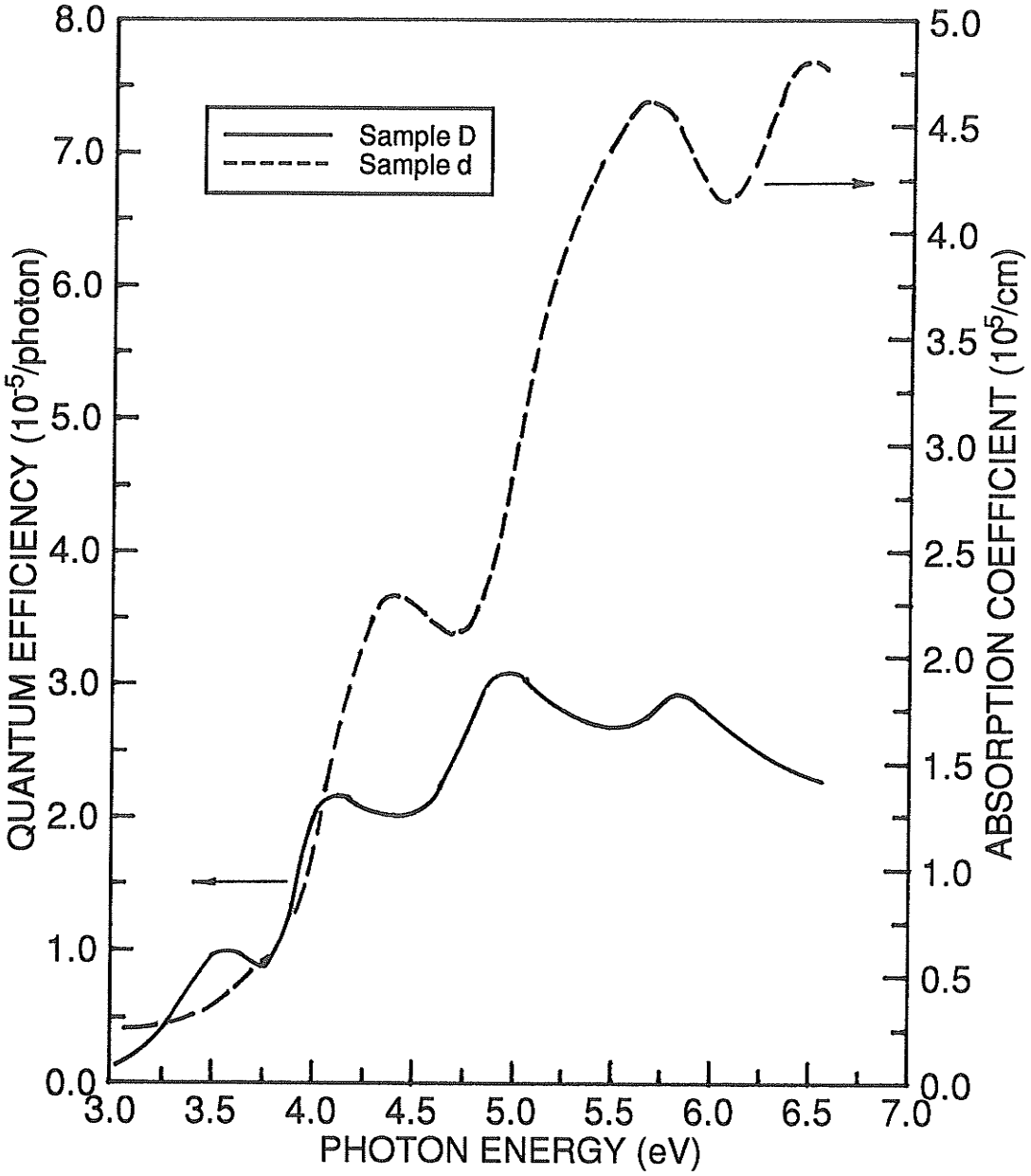

Figure 4.6: Comparison between the absorption spectra and the quantum efficiency spectra for fully cured polyimide samples d and D.

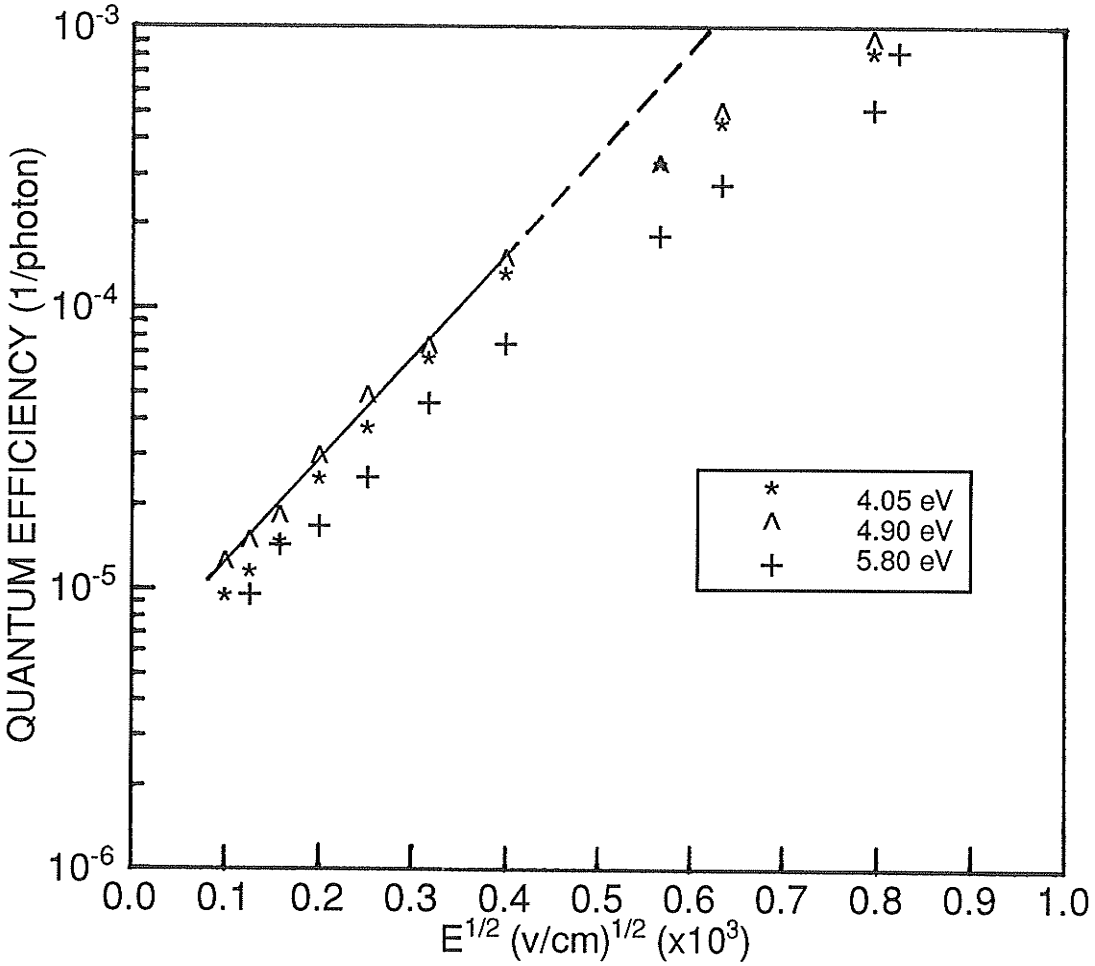

Figure 4.7: Plots of $\lg\Phi(E)$ versus E^2 at photon energies 4.05 eV, 4.90 eV and 5.80 eV for sample D.

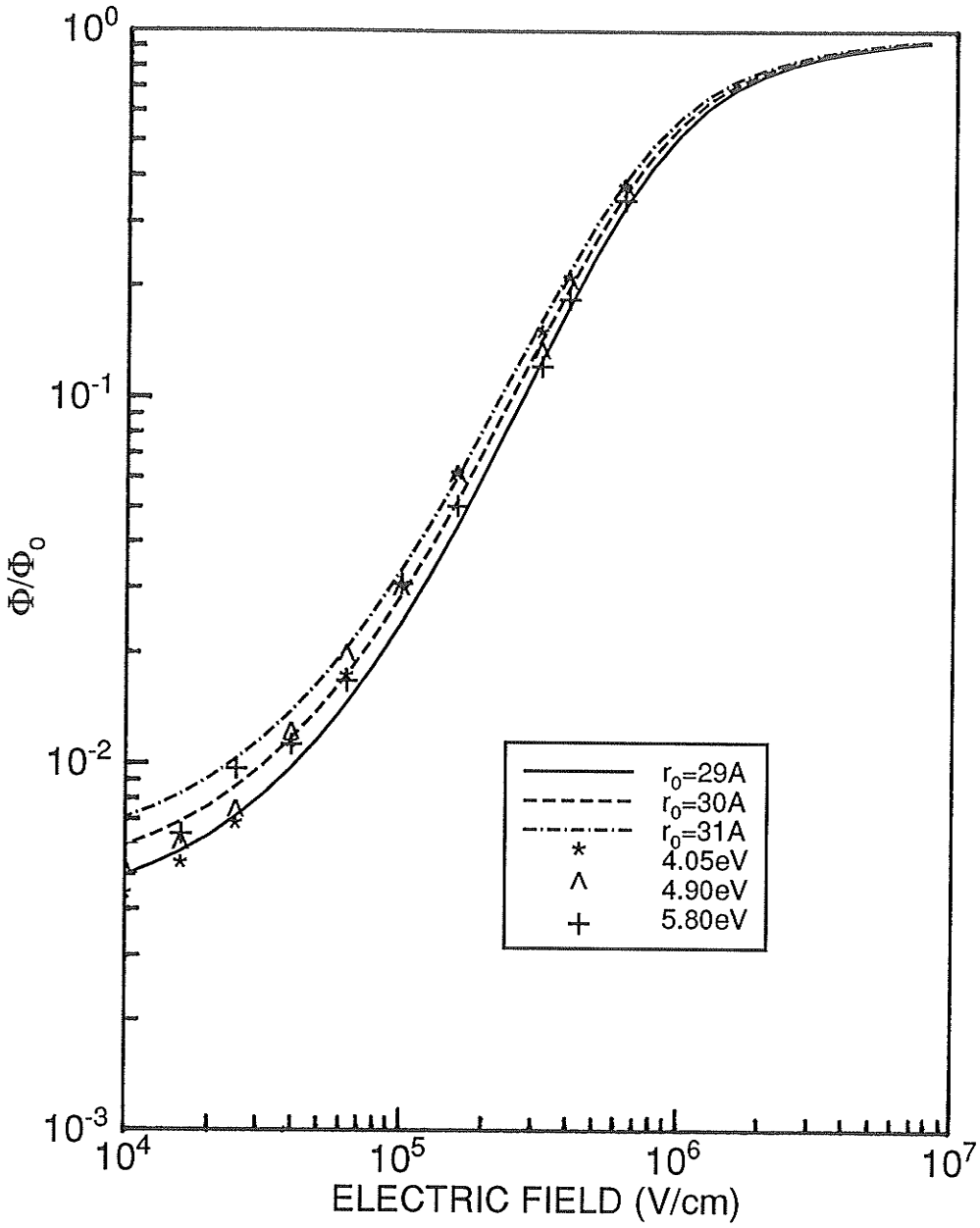

Figure 4.8: Photogeneration efficiencies of sample D plotted in Φ/Φ_o as functions of applied electrical field E with the primary yield Φ_o of 2.1×10^{-3} at 4.05eV, 2.4×10^{-3} at 4.90eV and 1.5×10^{-3} at 5.80eV. The curves were calculated from equ.(4.5) with r_o indicated in the figure.

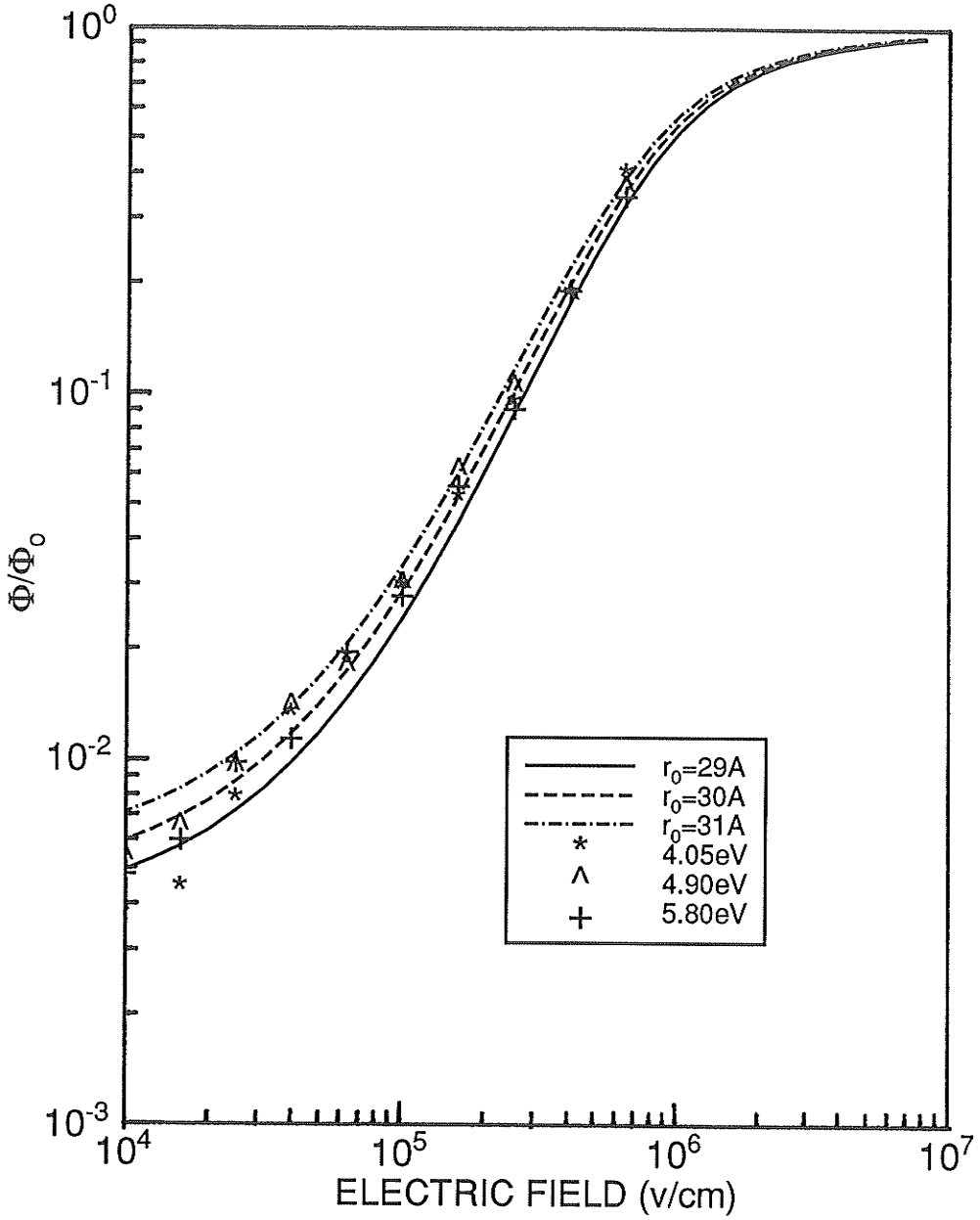

Figure 4.9: Photogeneration efficiencies of sample C plotted in Φ/Φ_o as functions of applied electrical field E with the primary yield Φ_o of 7.0×10^{-4} at 4.05eV, 7.4×10^{-4} at 4.90eV and 8.0×10^{-4} at 5.80eV. The curves were calculated from equ.(4.5) with r_o indicated in the figure.

Chapter 5

Conclusions

There are four ultraviolet absorption peaks and four corresponding photocurrent quantum efficiency peaks for the PMDA-ODA polyimide. The absorption peaks at 4.35 eV and 6.40 eV(corresponding to the quantum efficiency peaks at 4.05 eV and 5.80 eV) are due to the intramolecular transitions, and the absorption peaks at 3.65 eV and 5.65 eV(corresponding to the quantum efficiency peaks at 3.50 eV and 4.90 eV) are due to the intermolecular transitions. The photogeneration is a multiphoton process and is associated with the formation of charge-transfer(CT) complexes and the dissociation into free carriers under electrcal field and thermal stress. The experimental results follow well the Onsager theory. The photocurrent when the illuminated electrode is at the negative polarity is mainly caused by electron injection from the electrode. Effects of curing temperatures on absorption spectra and quantum efficiency spectra are mainly due to changes of molecular orders between dif-

ferent polyimide chains rather than to imidization.

REFERENCES

[1]. S.C. Freilich, Macromolecules 20, 973(1987)

[2]. R.A. Larson, IBM J. Res. Dev. 24, 286(1980)

[3]. A. Endo, M. Takada, K. Adachi, H. Takasago, T. Yada, and Y. Onishi, J. Electrochem. Soc. 134, 2522(1987)

[4]. E. Sugimoto, IEEE Electrical Insulation Magzine, 5, 15(1989)

[5]. *Electronic and Photonic Applications of Polymers*, edited by M. J. Bowden and S. R. Turner (American Chemical Society, Washington, 1988).

[6]. *Polymer Materials for Electronic Applications*, edited by E. D. Feit and C. W. Wilkins Jr. (American Chemical Society, Washington, 1982).

[7]. G. V. Treyz, R. Scarmozzino, and R. M. Osgood Jr., Appl. Phys. Lett., 55, 346(1988).

[8]. Y. Harada, F. Matsumoto, and T. Nakado, J. Electrochem. Soc., 130, 129(1983).

[9]. N. J. Chou, D. W. Dong, J. Kim, and A. C. Liu, J. Electrochem. Soc., 131, 2335(1984).

[10]. C. A. Kovac, J. L. Jordan-Sweet, M. J. Goldberg, J. G. Clabes, A. Vichbeck, and R. A. Pollak, IBM J. Res. Develop., 32, 1345(1988).

[11]. J. J. Pireaux, C. Gregorie, P. A. Thiry, R. Caudano, and T. C. Clarke, J. Vac. Sci. Technol., A 5, 598(1987).

[12]. M. J. Goldberg, J. G. Clabes, and C. A. Kovac, J. Vac. Sci. Technol., A 6, 985(1988).

[13]. B. D. Silverman, P. N. Sanda, P. S. Ho, and A. R. Rossi, J. Polym. Sci. Polym. Chem. Ed., 23, 2857(1985)

[14]. D. Ugolini, S. P. Kowalczyk, and F. R. McFeely, J. Appl. Phys., 72, 4912(1992).

[15]. W. R. Salaneck, CRC Crit. Rev. Solid State Mater. Sci., 12,267(1985).

[16]. J. L. Bredas and T. C. Clarke, J. Chem. Phys., 85, 253(1987).

[17]. S.A. Kafafi, J.P. LaFemina, and J.L. Nauss, J. Am. Chem. Soc. 112, 8742(1990)

[18]. S.P. Kowalczyk, S. Stafström, J.L. Brédas, W.R. Salaneck, and J.L. Jordan-Sweet, Phys. Rew. B 41, 1645(1990)

[19]. Y. Takai, M. M. Kim, A. Kurachi, T. Mizutani, and M. Ieda, Jpn. J. Appl. Phys., 21, 1524(1982).

[20]. *Photocurrent and Related Phenomena*, edited by J. Mort and D. M. Pai (Elsevier, New York,1976).

[21]. J.P. LaFemina, G. Arjavalingam, and G. Hougham, J. Chem. Phys. 90, 5154(1989)

[22]. T. Kubota, M. Iwamoto, and M. Sekine, IEEE Proc. 3rd Conf. PADM, 643(1991).

[23]. T. Rupp, M. Eberhardt, and H. Gruler, Jpn. J. Appl. Phys., 31, 3636(1992).

[24]. B. Chin and R. Tietze, Proc. NEPCON West'92, 3, 1763(1992).

[25]. D. Makino, IEEE Elec. Insulation Mag., 4, 15(1988).

[26]. W. A. Pliskin, J. Electrochem. Soc., 134, 2819(1987).

[27]. D. W. Hewak, F. Picard, and H. Jin, Proc. 1st Int. Workshop on Photonic Networks, 265(1991).

[28]. A. Husian, Microelectronic Interconnections and packaging: System Integration, SPIE Conf., 1390(1990).

[29]. J. I. Thackara, G. F. Lipscomb, M. A. Stiller, A. J. Ticknor, and R. Lytel, Appl. Phys. Lett. 52, 1031(1988).

[30]. G. F. Lipscomb, R. S. Lytel, A. J. Ticknor, T. E. Van Eck, S. L. Kwiatkowski and D. G. Girton, Nonlinear Optical Properties of Organic Materials III, SPIE COnf., 1337, 23(1990).

[31]. K. D. Singer, M. G. Kuzky, and J. E. Sohn, J. Opt. Soc. Am., B4, 968(1987).

[32]. S. Isoda, H. Shimada, M. Kochi, and H. Kambe, J. Polym. Sci. Polymer Phys. Ed., 19, 1293(1981).

[33]. J. W. Wu, E. S. Binkley, J. T. Kenney, and R. Lytel, Appl. Phys. Lett., 69, 7366(1991).

[34]. D. D. Denton, C. N. Ho, and S. G. He, IEEE Trans. Instrumentation and Measurement, 39, 508(1990).

[35]. R. Srinivasan and V. Mayne-Banton, Appl. Phys. Lett. 41,576(1982)

[36]. S.G. Hansen, J. Appl. Phys. 66, 1411(1989)

[37]. B.R. Hahn and D.Y. Yoon, J. Appl. Phys. 65, 2766(1989)

[38]. P.O. Hahn, G.W. Rubloff, and P.S. Ho, J. Vac. Sci. Technol. A2, 765(1984)

[39]. *Polyimides*, edited by K. L. Mittal(Plenum, New York, 1984)

[40]. L.B. Rothman, J. Electrochem. Soc. 127, 2217(1980)

[41]. L. Kan and K. C. Kao, J. Chem. Phys., 98, 3445(1993).

[42]. L. Kan and K. C. Kao, Proc. IEEE International Conf. on EI, 84(1990).

[43]. M. Navarre, in *Polyimides: Synthesis and Characterization*, edited by K. Mittal(Plenum, New York), 1984, pp.259.

[44]. C. Feger, J. Polym. Sci. Polym. Chem. Ed., 25, 2005(1987).

[45]. G. A. Pasteur, H. E. Bair, and F. Vratny, in *Thermal Analysis*, edited by B. Miller(Wiley-Heyden, Chichester), 1155(1982).

[46]. S. Isoda, H. Shimada, M. Kochi, and H. Kambe, J. Polym. Sci. Polym. Phys. Ed. 19, 1293(1981)

[47]. B.V. Kotov, Zh. Fiz. Khim. 62, 2709(1988) (in Russ.)

[48]. N. Takahashi, D.Y. Yoon, and W. Parrish, Macromolecules 17, 2583(1984)

[49]. C. Feger, Soc. of Plastic Engineers ANTEC Technical Papers, Los Angeles, 967(1987)

[50]. A. Endo and T. Yada, J. Electrochem. soc. 132, 155(1985)

[51]. H. M. Meyer, T. J. Wagner, J. H. Weaver, M. W. Feyereisen, and M. W. Almlof, J. Chem. Phys. Lett., 164, 527(1989).

[52]. E. D. Wachsman and C. N. Frank, Polymer, 29, 1191(1988).

[53]. B. L. Sharama and P. K. C. Pillai, Phys. Stat. Sol., 71(a), 583(1982).

[54]. K. Iida, M. Wakai, S. Nakamura, M. Ieda, and G. Sawa, Jpn. J. Appl. Phys. 23, 1573(1984)

[55]. H.J. Wintle, IEEE Trans. Electr. Insul. EI-12, 97(1977)

[56]. R.F. Chaiken and D.R. Kearns, J. Chem. Phys. 45, 3966(1966)

[57]. K.C. Kao and W. Hwang, *Electrical Transport in Solids* (Pergamon Press, Oxford, 1981), pp.404-436

[58]. S.T. Wellinghoff, H. Ishida. J.L. Koeing, and E. Baer, Macro molecules 13, 826(1980)

[59]. P.M. Borsenberger and A.I. Ateya, J. Appl. Phys., 49, 4035(1978)

[60]. P.J. Melz, J. Chem. Phys. 57, 1694(1972)

[61]. S. J. Fox, *Photoconduction in Polymers - An Interdisciplinary*

Approach(Technomic, Westport, CN), 1976, pp.253.

[62]. D. K. Davies, J. Phys. D, 5, 162(1972).

[63]. J. Frenkel, Phys. Rev., 54, 647(1938).

[64]. L. Onsager, Phys. Rev., 54, 554(1938).

[65]. D.M. Pai and R.C. Enck, Phys. Rev. B 11, 5163(1975)

[66]. A. Mozumder, J. Chem.Phys. 60, 4300(1974)

[67]. P. Meiz, Bull. Am. Phys. Soc., 17, 353(1985).

[68]. Rashimi, Y. Takai, T. Mizutani and M. Ieda, Jpn. J. Appl. Phys. 24, 1003(1985)

[69]. G. M. Sessler, B. Hahn, and D. Y. Yoon, J. Appl. Phys., 60, 318(1986).

[70]. K. Tahira and K. C. Kao, J. Appl. Phys., 18, 2247(1985).